Unraveling the molecular basis of *ao*, a maternal-effect gene in *Drosophila melanogaster*

Risa Takenaka

A dissertation
submitted in partial fulfillment of the
requirements for the degree of

Doctor of Philosophy

University of Washington
2024

Reading Committee:
Harmit S. Malik, Chair
Rick McLaughlin
M. K. Raghuraman

Program Authorized to Offer Degree:
Molecular and Cellular Biology

University of Washington

Abstract

Unraveling the molecular basis of *ao*, a maternal-effect gene in *Drosophila melanogaster*

Risa Takenaka

Chair of the Supervisory Committee:
Harmit S. Malik
Department of Genome Sciences

The *abnormal oocyte* (*ao*) gene of *Drosophila melanogaster* is a maternal-effect, embryonic semi-lethal gene located on the left arm of the 2nd chromosome. *ao* was recovered from a wild *D. melanogaster* population and initially described by Larry Sandler and colleagues in 1968. Subsequent studies found that increasing heterochromatic regions on the X, Y, and 2nd chromosomes rescued the maternal-effect lethality of *ao*. For over 20 years, *ao* has been presumed to be a transcriptional regulator of core histones. However, the two existing *ao* mutant strains carry background mutations, and one of the strains is no longer available. We, therefore, created a CRISPR/Cas9-mediated knockout of the *ao* allele to separate the *ao* phenotype from background effects. Using the Δ*ao* flies, we found that although *ao* mutants exhibit maternal-effect lethality that is ameliorated by a reduction in histone copy number, *ao* does not affect histone transcript levels as previously reported. Given that Ao's plant and mammalian orthologs are E3 ligases, we hypothesized that Ao is also an E3 ligase and used proteomics approaches to identify its potential targets. Finally, by maintaining the Δ*ao* flies as homozygous stocks, we

allowed the strains to evolve *de novo* suppressors of the maternal-effect phenotype and used whole-genome sequencing to identify genomic changes associated with the loss of the *ao* maternal-effect lethality phenotype. Although our findings challenge the published molecular model of *ao* as a histone-transcript suppressor, we did find evidence for *ao*'s genetic interaction with histones. Understanding the basis of *ao*-associated maternal-effect lethality and its connection to histone copy number and heterochromatin remains an open and exciting question.

ACKNOWLEDGEMENTS

Thanks to my advisor, Harmit Singh Malik. I often make regrettable choices, but I stand by my decisions to come to UW, rotate in your lab, and join your lab. Some people earn their PhDs in spite of their advisors. I made it to the end because of you.

Thanks to the Malik lab, in all its iterations. The 2019 lab for welcoming me with open arms; the 2020 to 2023 versions for being my home; and the 2024 cohort for being a group that I will miss sorely. A special thanks to Aida de la Cruz and Janet Young for your support, both material and ephemeral, not to mention scientific; to Courtney Schroeder, Ching-Ho Chang, and Pravrutha Raman for your scientific mentorship and companionship at the scope; and to Sierra Simmerman for running to the finish line with me.

Thanks to my Atlanta collaborators Leila Rieder, Casey Schmidt, and Eric Albanese. A special thanks to Casey for working through this puzzle with me, and for your unflappability and generosity under fire. Thanks to Phil Gafken, Brian Milless, and Chenwei Lin for making possible the proteomics experiments. Thanks to Aravind Iyer, who provided us with detailed bioinformatics analyses of the DET1 protein. Thanks to all those who came before me who made this dissertation possible: Dan Lindsley, Maria Berloco, Sergio Pimpinelli, Bill Sullivan, and John Tomkiel, among others. And a most special thanks to the OG, Larry Sandler.

Thanks to my wonderful thesis committee: Akhila Rajan, Daniel Promislow, Rick McLaughlin, M.K. Raghuraman, and Michael Ailion. I am grateful for your rigor and support, and for your grace during a certain portion of my general exam involving the natural history of ducks. Additional thanks to my reading committee, Raghu and Rick: to Raghu for demonstrating true pedagogy, both as the instructor for my TAship and committee member, and to Rick for giving me the best introduction to grad school. The decision to choose my permanent lab was the hardest one I had to make as a grad student; thank you for your honesty and for steering me right.

Thanks to my parents for all the love and support over the years, and for establishing a life for us in the US. This degree would not have been possible without your sacrifice. Mom, thank you for being my biggest champion in pursuing this degree. Thanks also, of course, to my grandparents. I hope this PhD makes you proud.

Thanks to my friends (*H. sapiens*): Jessica for the perspectives and always fun times; Alexis for showing me the way and the chats deep and inane, whenever and wherever; Katharine, my phone-a-friend, for the countless happy hours in the sun and rain; and Rachel for the steadfast friendship through 3 cities and decades of life.

Thanks to my friends (*F. catus*): Harry, cat-in-disguise, for raising me; Moira for reminding me of the importance of embracing your quirks and teaching me to leap into joy; Pickle for showing me that it's ok to take your time; Wendell, my baby boy, for your absolute sweetness; Sadie for planting the seed. Finally, infinite thanks and love to Sophie, my best friend and raison d'être of my Seattle years. You magnificent creature, you. This one is for you.

DEDICATION

This dissertation is dedicated to the memory of Sophie Case (2005-2023).

TABLE OF CONTENTS

Chapter 1: Introduction

1.1	A brief history of *abnormal oocyte* (*ao*)	1
1.2	The AO heterochromatin: a remedy for the *ao* maternal-effect lethality	2
1.3	Mapping and identifying the *ao* mutation	4
1.4	*ao* as a negative regulator of core histones	4
1.5	Dissertation overview	6

Chapter 2: *ao* is not a negative regulator of histones

2.1	Abstract	8
2.2	Introduction	8
2.3	Results	9
2.4	Discussion	20
2.5	Materials and methods	22
2.6	Acknowledgements	28

Chapter 3: Ao as an E3 ligase

3.1	Abstract	29
3.2	Introduction	29
3.3	Results	31
3.4	Discussion	39
3.5	Materials and methods	42
3.6	Acknowledgements	44

Chapter 4: Suppressors of *ao*

4.1	Abstract	45
4.2	Introduction	45
4.3	Results	47
4.4	Discussion	53
4.5	Materials and methods	54
4.6	Acknowledgements	55

Chapter 5: Perspectives and prospectives

5.1	Dissertation summary	56
5.2	Future directions	58

Appendix

A1	RNA-seq	60
A2	Positive selection of *Drosophila ao*	63

References 67

LIST OF FIGURES

Figure 1.1	AO heterochromatic elements	2
Figure 1.2	A model for *ao* rescue by AO heterochromatin	3
Figure 1.3	The *ao* gene	4
Figure 2.1	Schematic of the CRISPR/Cas9-mediated *ao* knockout	10
Figure 2.2	Fertility assay of Δ*ao* flies	11
Figure 2.3	Generation and validation of the *ao*-transgene rescue construct	13
Figure 2.4	Generation and validation of the *ao-V5* flies	14
Figure 2.5	The Ao protein localizes to the histone gene cluster in ovaries	15
Figure 2.6	*ao* does not affect histone transcript levels	16
Figure 2.7	Relationship between *ao* and histone copy number	18
Figure 2.8	Excess Y chromosome rescues the Δ*ao* maternal-effect lethality	19
Figure 3.1	Proteins identified in pull-down mass spectrometry using *ao-HA* ovaries	32
Figure 3.2	Proteins identified in TMT mass spectrometry with Δ*ao* ovaries	35
Figure 3.3	Western blots for H2B and H3 on Δ*ao* and wildtype ovaries	39
Figure 4.1	Fertility assay on Δ*ao* lines kept in homozygous stocks	48
Figure 4.2	X^Y cross on Δ*ao* lines kept in homozygous stocks	49
Figure 4.3	No change in histone copy number in lines with suppressor phenotypes	51
Figure 4.4	No change in rDNA copy number in lines with suppressor phenotypes	52
Figure A1.1	Differentially expressed genes (Δ*ao*/WT) from poly(A) RNA-seq	61
Figure A2.1	Illustration of the McDonald-Kreitman test	63
Figure A2.2	Fertility assay of Δ*ao* flies with the *D. simulans ao* transgene	65

LIST OF TABLES

Table 2.1	Core histone transcript levels from ribo-depletion RNA-seq analysis	17
Table 2.2	Primer sequences used in Chapter 2	27
Table 3.1	Proteins identified in pull-down MS with $\log_2(FC) > 1.0$, FDR < 0.10	33
Table 3.2	Proteins identified in the yeast two-hybrid assay	34
Table 3.3	Proteins identified in TMT MS with $\log_2(FC) > 1.0$, FDR < 0.05	36
Table 3.4	Proteins identified in TMT MS with $\log_2(FC) < -1.0$, FDR < 0.05	36
Table 3.5	Core histones identified in TMT MS	38
Table 3.6	Variant histones identified in TMT MS	38
Table 3.7	Core and variant histones identified in pull-down MS	38
Table A2.1	McDonald-Kreitman test on Ao	64

Chapter 1: Introduction

1.1: A brief history of *abnormal oocyte* (*ao*)

In October of 1965, Larry Sandler, together with colleagues Dan Lindsley, Benedetto Nicoletti, and Gianni Trippa, ventured to a fruit market in Rome, Italy, and later to a winery in the outskirts of town, to collect fruit flies. This fieldwork was the fruit of Sandler and Lindsley's joint sabbatical proposal, in which they had explained their motivation to screen wild populations of *Drosophila melanogaster* for recessive mutations affecting meiosis. This proposal had been inspired by studies Sandler had conducted with Yuichiro Hiraizumi on *Segregation Distorter*, a meiotic-drive gene complex that was isolated from a natural *D. melanogaster* population in Madison, Wisconsin (Sandler et al. 1959, Ganetzky 1999, Lindsley 1999). Lindsley recounted that Sandler, owing to his "ineptitude with an insect net" and near-fluent Italian, took on the task of reassuring curious onlookers about the legitimacy of their fieldwork, whereas Lindsley worked the insect net around market stalls. Only later did he find out that Sandler had not explained to the astonished shoppers and shopkeepers that Lindsley was a geneticist collecting samples for scientific research but that he was chaperoning this strange but mostly harmless American as he went about with his peculiar antics (Lindsley 1999)[1].

Among the chromosomes isolated from their Roman fieldwork was one that produced an excess of female offspring when mated to males carrying an attached X^Y chromosome (Sandler et al. 1968, Sandler 1970). Sandler named this mutant *abnormal oocyte* (*ao*) for its aberrant sex-ratio phenotype (Sandler 1970)[2]. *ao* is a maternal-effect gene; the maternal genotype has a causal influence on the offspring phenotype (Wolf and Wade 2009). These genes often encode products that are critical for early development, when the zygotic genome is inactive and embryonic development depends on maternal gene products (Schier 2007). A subsequent analysis by Sandler showed that *ao* was one of five maternal-effect, embryonic semi-lethal genes located on the left arm of the 2nd chromosome (Sandler 1977). These five genes shared the unusual property that survival of offspring from homozygous-mutant mothers increased with an increase in the

[1] I've paraphrased this vignette, but Lindsley recounted that Sandler, his "closest scientific colleague," also was never one to "let his desire to cover the subject get in the way of a good story" (Lindsley 1999).
[2] The original three-letter abbreviation of this gene, unbeknownst to American Drosophilists, is a slur against Aboriginal people in Australia. At the time of this writing this dissertation, we are in the official process of making a nomenclature change to *ao* (pronounced ay-oh, à la Freddie Mercury).

amount of X and Y heterochromatin in the zygote (Sandler 1977). These genes promised to reveal the mechanistic basis of genetic interactions between euchromatin, heterochromatin, and embryonic viability.

1.2: The AO heterochromatin: a remedy for the *ao* maternal-effect lethality

Research on *ao* in the following two decades bolstered Sandler's initial observation that the viability of offspring from *ao* mutant mothers could be rescued by increasing the dosage of certain heterochromatic regions on the X, Y, and 2nd chromosomes (Parry and Sandler 1974, Sandler 1977, Haemer 1978, Yedvobnick et al. 1980, Pimpinelli et al. 1985, Tomkiel et al. 1991). These regions, located on the distal heterochromatin on the X, the long and short arms of the Y (the *Drosophila* Y chromosome is entirely heterochromatic), and the centromeric heterochromatin on the right arm of the 2nd chromosome, were named AO heterochromatic elements (Fig 1.1; Pimpinelli et al. 1985).

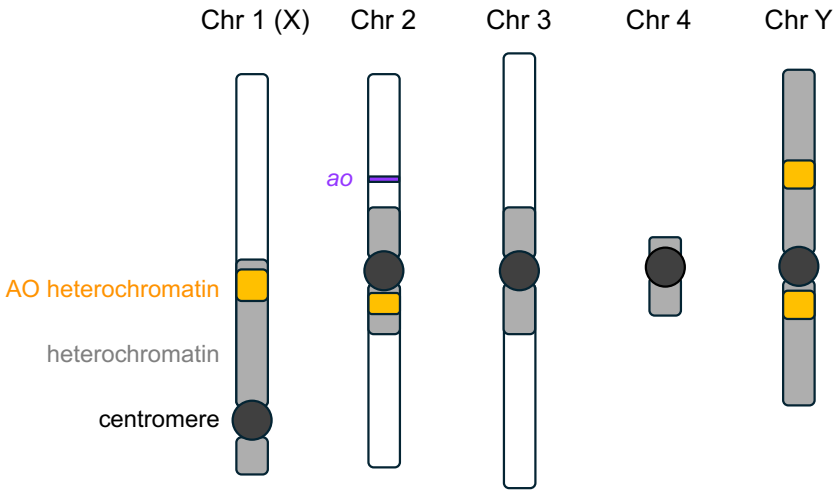

Figure 1.1: AO heterochromatic elements, located on the X, Y, and 2nd chromosomes and denoted in orange, contain elements that rescue the *ao* maternal-effect lethality.

The mechanistic relationship between the *ao* mutation and AO heterochromatin remained (and remains) unclear. Sandler hypothesized that given 1) the location of the ribosomal DNA (rDNA) locus on the X heterochromatin, and 2) the decrease in the degree of maternal-effect lethality at 19.5°C compared to 25.5°C (flies develop slower at lower temperatures), increase in the rDNA copy number (or the number of rDNA repeats at the locus) was responsible for AO

heterochromatin's amelioration of the maternal-effect lethality. Indeed, a subsequent study found that *ao* mutant flies maintained in a homozygote stock developed an expansion of the rDNA locus that alleviated the maternal-effect lethality (Krider and Levine 1975). Later studies observed the same suppressor phenotype in *ao* flies kept in homozygote stocks. However, while some found additional evidence implicating rDNA (Krider et al. 1979; Graziani et al. 1981), others disputed that rDNA copy number was the cause for the suppressor phenotype (Yedvobnick et al. 1980, Pimpinelli et al. 1985, Sullivan and Pimpinelli 1986, Manzi et al. 1986, Cavaliere et al. 1991).

Furthermore, it remained (and remains) unclear whether AO heterochromatin rescues the *ao* mutation directly (i.e, both *ao* and AO produce the same product) or indirectly (i.e., the AO product is different from *ao*'s, but performs a rescue function). Based on the latter hypothesis, Bill Sullivan, who completed his doctoral thesis under Larry Sandler's supervision at the University of Washington, proposed a "sink" model for the relationship between the *ao* mutation and AO heterochromatin (Sullivan 1985). According to this hypothesis, a mutation in *ao* leads to the overproduction of an (unknown) transcript or protein ("Factor X") that causes the maternal-effect lethality of *ao* mutant mothers. The AO heterochromatin acts as a sink or sponge for the deleterious Factor X, lowering its overall amount and thereby alleviating the maternal-effect lethality (Sullivan 1985). This model provided an elegant explanation for the relationship between the *ao* mutant phenotype and its rescue via AO heterochromatin.

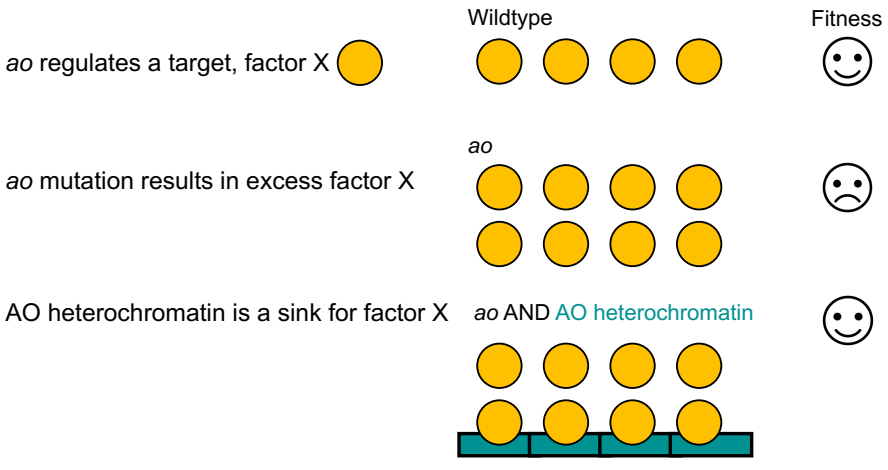

Figure 1.2: A model for *ao* rescue by AO heterochromatin proposed by Bill Sullivan (1985). The AO heterochromatin acts as a sink to quench the deleterious excess products ("factor X") produced in the absence of *ao*.

1.3: Mapping and identifying the *ao* mutation

Despite over two decades worth of research on *ao,* it wasn't until 1995 that John Tomkiel and colleagues mapped the *ao* mutation to locus 32C on the 2nd chromosome (Tomkiel et al. 1995). The genetic unmasking of *ao* took advantage of two *ao* mutants (ao^1, the 2nd chromosome isolated from the Roman fruit-market flies, and ao^2, a *P*-element induced allele) and a transgenic rescue construct (Tomkiel et al. 1995).

In 2001, Maria Berloco and colleagues identified *ao* as the *D. melanogaster gene CG6093* (Berloco et al. 2001). *ao* was defined as a 1,974-bp sequence producing a 1.8-kilobase transcript, which encoded the 509-amino acid Ao protein (Fig 1.3; Berloco et al. 2001). They also identified *ao* as the *D. melanogaster* ortholog of the *de-etiolated* (*DET1*) gene, first characterized in *Arabidopsis thaliana* but later shown to be present in other plants and animals (Berloco et al. 2001, Chory et al. 1989). Finally, this study proposed a molecular mechanism underlying *ao*'s maternal-effect lethality: the authors reported that *ao* acts as a transcriptional regulator of core histones and concluded that the excess histones in eggs from *ao* mutant mothers resulted in the *ao* maternal-effect lethality (Berloco et al. 2001).

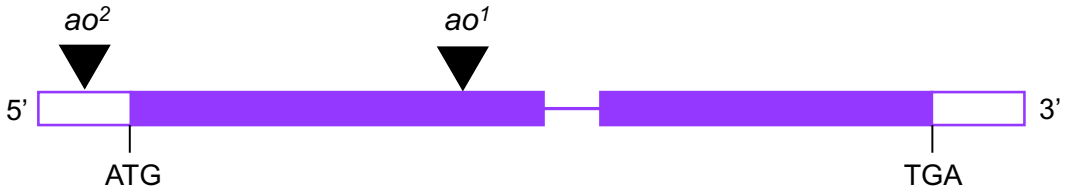

Figure 1.3: The *ao* gene, located on the left arm of the 2nd chromosome (cytogenic locus 32C), is a 1,974-bp sequence interrupted by a single intron. ao^1 has a *Doc* transposable element insertion in the coding sequence. ao^2 has a *P*-element insertion in the 5'UTR.

1.4: *ao* as a negative regulator of core histones

Core histones (H2A, H2B, H3, and H4) and the linker histone (H1) of *D. melanogaster* are arranged in a tandemly repeated, multigene array of approximately 100 units on the 2nd chromosome (for a total of approximately 200 copies of the histone units per diploid fly); the exact copy number varies among and within *Drosophila* species (Lifton et al. 1978, Strausbaugh and Weinberg 1982, Kremer and Hennig 1990, McKay et al. 2015, Shukla et al. 2024). Although

new transgenic tools have begun to overcome the challenge of manipulating histone copy numbers (e.g., Cook et al. 2012, McKay et al. 2015, Zhang et al. 2019), the tight regulation of histone expression still makes it challenging to manipulate histone levels in *Drosophila*. For example, Dan McKay and colleagues demonstrated that flies carrying 24 copies of histone genes have nearly identical levels of histone transcripts and proteins as wildtype flies with 200 copies of histone genes (McKay et al. 2015), likely due to a feedback-based compensation mechanism that ensures adequate histone expression levels regardless of histone gene copy number (McKay et al. 2015). Thus, *ao* has been a valuable tool for *Drosophila* researchers in the quest to manipulate histone gene expression (e.g., Chari et al. 2019).

A series of complementary experiments established the relationship between *ao* and histone genes (Berloco et al. 2001). First, the authors raised a polyclonal antibody against the Ao protein to determine Ao's localization and binding patterns. They found (via immunostaining) that the Ao protein colocalized with the histone genes (via *in situ* hybridization) in both polytene chromosomes from larval salivary glands and mitotic chromosomes from larval neuroblasts. They observed the same colocalization pattern in the *D. melanogaster* sister species *D. simulans* and the more distantly related *D. virilis.* Next, using the same Ao antibody, they performed an X-ChIP (cross-linking chromatin immunoprecipitation) experiment and found that the Ao protein binds to the promoter regions of core histones (H2A, H2B, H3, H4) in 0-to-4-hour embryos, and additionally to the H1 promoter in *D. melanogaster* SL-2 cells, derived from 20-to-24-hour embryos (Schneider 1972).

Given these data, Berloco and colleagues tested the hypothesis that Ao might be a transcription factor for histone genes. Based on Northern blotting analyses, they found that unfertilized eggs from ao^1/ao^2 trans-heterozygous females had a 1.6-fold (for histone H4) to 11-fold (for histone H2A) increase in core histone transcripts relative to unfertilized eggs from wildtype Oregon-R females (Berloco et al. 2001). Eggs from heterozygous *ao* females (both ao^1 and ao^2) had histone transcript levels comparable to wildtype eggs. In an elegant final experiment, the authors tested the relationship between *ao* and histone copy number *in vivo*: they compared the fertility of *ao* females with wildtype histone copy numbers against *ao* females with a heterozygous deletion of the 2nd chromosome corresponding to the histone gene locus. Remarkably, they found that the relative survival for offspring from *ao* females with histone deficiencies was 40% compared to

the 20% survival rate for *ao* females with wildtype histone copy numbers. (Survival rate was calculated as the ratio of adult offspring to eggs laid; relative survival was then calculated as the ratio of the relative survival of *abo* mutants compared to the heterozygous control.) Thus, they found that reducing the histone copy number in ao^1-mutant flies partially ameliorated the maternal-effect lethality associated with *ao* mutants (Berloco et al. 2001).

These findings led Berloco and colleagues to the model that excess histones in *ao*-mutant females cause the maternal-effect lethal phenotype. According to this model, core histones represented the hitherto unknown "Factor X" in Bill Sullivan's heterochromatin-as-a-sink model (Sullivan 1985). The authors of the 2001 paper suggested that increasing doses of AO heterochromatin could titrate out the excess histones produced by *ao*-mutant mothers, thereby alleviating embryonic lethality (Berloco et al. 2001). Thus, this landmark study connected the function of *ao*, a euchromatic gene that controls histone gene expression, with heterochromatin content and, ultimately, embryonic viability.

1.5: Dissertation overview

With the mechanism of *ao*'s maternal-effect lethality established, subsequent studies utilized the *ao* mutant as a tool to interrogate the effects of histone overexpression in *D. melanogaster* (e.g., Chari et al. 2019). Because the *ao* phenotype is restricted to ovaries (i.e., maternal-effect lethality, with no other defects in mutant flies), *ao* promised to be an exciting tool to interrogate the tissue-specific responses of histone overexpression in a multicellular organism.

Despite *ao*'s promise as an experimental tool for histone overexpression, existing *ao* reagents had several associated caveats. First, of the two *ao* strains used historically, only the ao^1 strain is still available; the ao^2 stock has been lost. The ao^1 stock is derived from the 2nd chromosome isolated from the wild population in Rome (Sandler et al. 1968). The ao^1 mutation results from an incomplete *Doc* transposable element insertion in the first exon, leading to a larger transcript relative to wildtype *ao* (Fig 1.3; Berloco et al. 2001). The ao^2 allele was generated in the lab via *P*-element mutagenesis (Tomkiel et al. 1995). The ao^2 mutation had a $P[ry^+]$ insertion into the *ao* promoter region and produced no detectable transcripts (Fig 1.3; Berloco et al. 2001).

Moreover, the two *ao* mutants differed with respect to a key phenotype: whereas ao^1 is viable as a homozygous mutant, ao^2 was lethal as a homozygote (Tomkiel et al. 1995). Although both ao^1/ao^1 and ao^1/ao^2 mutants exhibited maternal-effect lethality, a greater percentage of embryos from ao^1/ao^1 mothers died at earlier stages compared to those from ao^1/ao^2 mothers, which was attributed to a fertilization defect in eggs from ao^1/ao^1 mothers (Tomkiel et al. 1995). These results implied that genetic background effects could dramatically affect the severity of the phenotype associated with loss of *ao*.

To overcome these challenges, I created a clean *ao* knockout using CRISPR/Cas9. Using the *ao*-knockout flies, I found that contrary to prior evidence, *ao* is not a transcriptional repressor of core histones (Chapter 2). I explored the possibility that *Drosophila ao*, like its plant and mammalian orthologs, could also encode a subunit of an E3 ubiquitin ligase, and identified the *Drosophila* separase Three rows as a potential target of Ao (Chapter 3). Finally, by maintaining the Δ*ao* flies as homozygous stocks, I allowed the strains to evolve *de novo* suppressors of the maternal-effect phenotype and used whole-genome sequencing to identify genomic changes associated with the loss of the *ao* maternal-effect lethality phenotype (Chapter 4).

Chapter 2: *ao* is not a negative regulator of histones

2.1: Abstract

The *abnormal oocyte* (*ao*) gene of *Drosophila melanogaster* is a maternal-effect lethal gene, which was identified as encoding a transcriptional regulator of core histones (Berloco et al. 2001). Despite *ao*'s promise as a tool to interrogate the effects of histone overexpression, existing *ao* mutant strains likely carry background mutations. To distinguish the true *ao* phenotype from background effects, we created two new *ao* reagents: a CRISPR/Cas9-mediated knockout of the *ao* allele for genetic and molecular analyses, and an *ao* allele tagged with the V5 epitope for cytological and potentially proteomic experiments. Using these reagents, we confirm that *ao* exhibits maternal-effect lethality that can be rescued by either a decrease in the histone copy number or an increase in heterochromatin on the Y chromosome and that the Ao protein localizes to the histone gene array in ovaries. However, contrary to the prior report, we find that *ao* does not repress core histone transcripts. Our data suggest that although *ao* interacts with the histone genes and heterochromatin as previously suggested, the molecular mechanism that underlies these interactions still remains to be elucidated.

2.2: Introduction

More than three decades after its initial description, *ao* was characterized as a transcription factor regulating the expression of core histone transcripts (Berloco et al. 2001). This finding made *ao* a promising tool for manipulating histone levels in *D. melanogaster*. However, existing *ao* reagents have several caveats. First, only the ao^1 strain is still available, whereas the ao^2 strain has been lost. Second, the two mutants exhibit different phenotypes: ao^1 is viable as a homozygous mutant, but ao^2 was lethal as a homozygote (Tomkiel et al. 1995). Furthermore, although both ao^1/ao^1 and ao^1/ao^2 mutants exhibited maternal-effect lethality, more embryos from ao^1/ao^1 mothers died at earlier stages compared to those from ao^1/ao^2 mothers (Tomkiel et al. 1995). Finally, ao^1/ao^1 stocks are unstable and have been known to acquire genetic suppressors that alleviate the maternal-effect lethality (Krider and Levine 1975, Graziani et al. 1981, Manzi et al. 1986). These results implied that genetic background effects could dramatically affect the severity of the phenotype associated with loss of *ao*.

To overcome these hurdles, and to accurately characterize the *ao* phenotype, we used CRISPR/Cas9-based methods to generate two new *ao* reagents. The first of these is a precise knockout of *ao* to enable downstream genetic analyses. The second reagent is a V5 epitope-tagged version of *ao* at the endogenous locus for cytological visualization. Using these reagents, we recapitulated several of the classical genetic attributes of *ao*, including its maternal-effect lethality, which is suppressed either by a reduction in histone gene copy number or by excess heterochromatin. We also found that the Ao protein localizes to the histone gene cluster, consistent with previous reports. However, contrary to prior evidence, we found that *ao* does not affect histone transcript levels. Unlike in ao^1/ao^2 flies, histone levels are unaffected in ovaries from both Δ*ao*/Δ*ao* and ao^1/ao^1 homozygous females. Thus, although *ao* does genetically interact with histones and heterochromatin, consistent with Sandler's original hypothesis, we conclude that the molecular basis for these interactions remains unknown.

2.3: Results

Δ*ao*-knockout flies have partial maternal-effect lethality

To obtain an *ao* mutant without associated genetic background effects, we used CRISPR/Cas9 to create a Δ*ao* strain. We designed guide RNAs to target the start of the 5' UTR and end of the 3' UTR of *ao* (Fig 2.1). To facilitate phenotypic screening of Δ*ao* flies, we inserted a repair template with the fluorescent marker *dsRed* under control of the eye-specific promoter *3xP3* using homology arms of approximately 1000 base pairs. We verified the *ao* knockout and *dsRed* replacement using PCR and Sanger sequencing (Fig 2.1). We also generated a strain that is nearly isogenic to the yw; Δ*ao/CyO-gfp* strain except for a wildtype 2nd chromosome in place of Δ*ao*, and used these flies as the wildtype control for all future experiments.

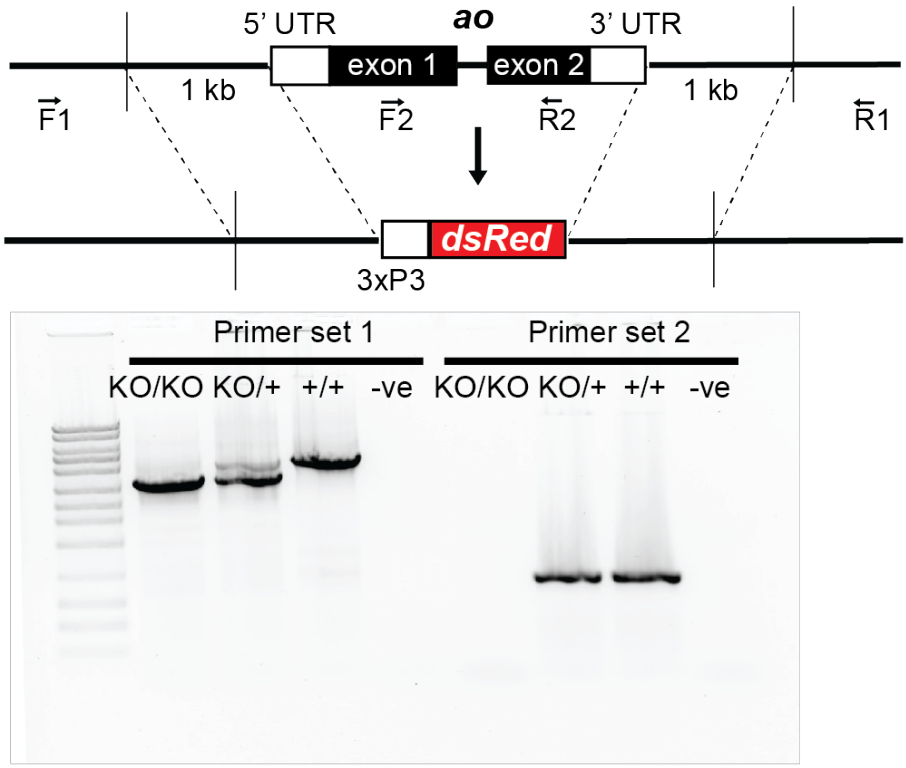

Figure 2.1: Schematic of the CRISPR/Cas9-mediated *ao* knockout. The *ao* coding sequence and UTRs were replaced with *dsRed* (fluorescent marker) under the control of *3xP3*, an eye-specific promoter. The repair template sequence included homology arms spanning approximately 1kb upstream and downstream of the *ao* coding sequence. The *ao* (1851 bp) knockout and *3xP3-dsRed* (903 bp) replacement were confirmed with PCR using two sets of primers. Primer set 1 (F1, R1) is external to the repair template. The expected wildtype and *dRed* and for primer set 1 is 4139 bp and 3191 bp, respectively (heterozygotes have both bands). The expected wildtype band for primer set 2 (F2, R2), which lies within the *ao* coding sequence, is 883 bp.

We first assessed whether our newly generated Δ*ao* strain recapitulated the characteristic partial maternal-effect lethality phenotype of *ao* mutants (Sandler 1970, Sandler 1977, Tomkiel et al. 1995). The degree of *ao*-associated maternal-effect lethality was reported to be more pronounced at higher temperatures (Sandler 1970). Therefore, we performed fertility assays with Δ*ao* flies at 29°C. Consistent with previous findings, we found that Δ*ao* females exhibit partial maternal-effect lethality when crossed to wildtype males (Fig 2.2A). We found that maternal-effect lethality is exacerbated in crosses between Δ*ao* females and Δ*ao* males, confirming previous findings that a paternal copy of the wildtype *ao* allele can rescue zygotic survival (Fig 2.2A; Pimpinelli et al. 1985, Tomkiel et al. 1995). Although our data suggested a slight fertility increase of Δ*ao* males relative to wildtype males in crosses with wildtype females (Fig 2.2A), subsequent experiments revealed no significant differences in these crosses (Fig 2.2B).

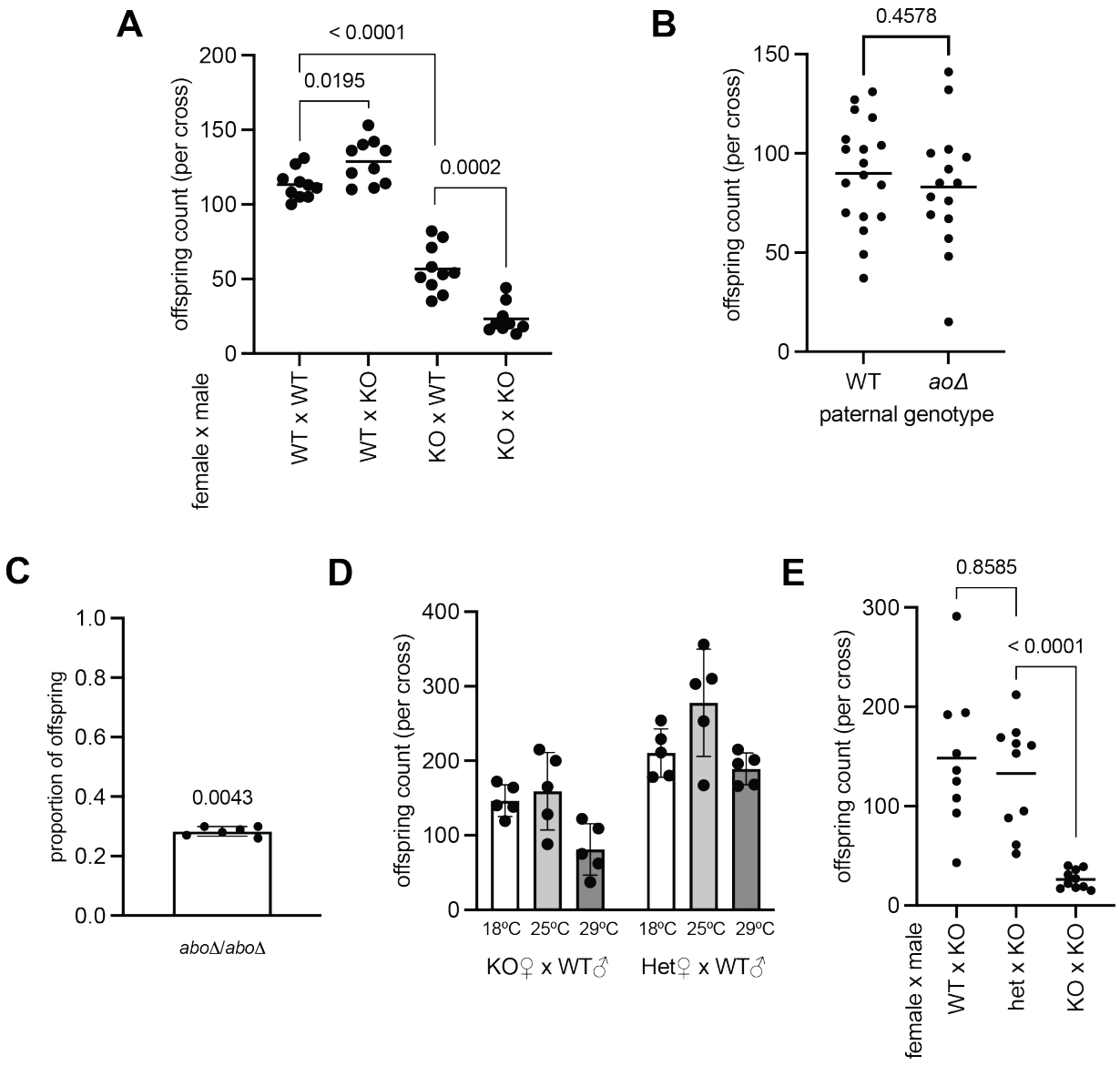

Figure 2.2: Fertility assay of Δ*ao* flies. Each point on a graph is the offspring count from a biological-replicate cross. All crosses plotted on one graph were set up, flipped, and counted on the same days. **A) Δ*ao* flies exhibit maternal-effect lethality.** Crosses were set up and maintained at 29°C. KO is Δ*ao*, WT is the isogenic *yw* strain with wildtype *ao*. *p*-values from two-tailed Mann-Whitney U tests are shown above brackets connecting the compared samples. **B) Δ*ao* flies do not exhibit paternal-effect lethality.** Crosses were set up and maintained at 25°C. Males were mated to Oregon R females; the WT male is also Oregon R. *p*-values are from two-tailed Mann-Whitney U tests. **C) Offspring from heterozygous Δ*ao* parents show a mild zygotic effect.** Crosses were set up and maintained at 25°C. **D) The maternal-effect lethality of Δ*ao* females is most pronounced at 29°C.** Crosses for each temperature were set up, flipped, and counted on the same days. KO is Δ*ao*, het is Δ*ao*/+, and WT is Oregon R. **E) Heterozygous Δ*ao* females have wildtype fertility.** Crosses were set up and maintained at 29°C. All crosses were set up, flipped, and counted on the same days. KO is Δ*ao*, het is Δ*ao*/+, and WT is the isogenic *yw ao*. *p*-values are from two-tailed Mann-Whitney U tests.

We further assessed zygotic effects in Δ*ao* flies by looking for deviations from the Mendelian ratio in offspring genotypes. In the absence of a zygotic effect, the theoretical Mendelian ratio for offspring from two heterozygous parents is 33% Δ*ao* homozygotes and 66% heterozygotes (homozygous balancers are lethal). The offspring genotype from parents heterozygous for Δ*ao* was 28% homozygous and 72% heterozygous, indicating a mild, but statistically significant, zygotic effect (Fig 2.2C). Our findings of *ao*-associated maternal-effect lethality are most pronounced at 29°C, but also manifest at 25°C and 18°C, albeit to slightly lower extents (Fig. 2.2D; Sandler 1970). Finally, as previously reported, we found that heterozygous females with one copy of the Δ*ao* allele have wildtype fertility (Fig 2.2E; Sandler 1970). Thus, the Δ*ao* strains we created confirm previous findings from ao^1 *and* ao^2 strains: loss of *ao* results in no deleterious consequences to paternal fertility but does cause maternal-effect lethality, which can be partially rescued by a wildtype paternal allele of *ao* in the zygote.

To rule out the possibility that the maternal-effect lethality in Δ*ao* strains might have resulted from an off-target mutation introduced during the CRISPR/Cas9 cleavage or repair, we generated a 'rescue' *ao* transgene (Fig 2.3A). We used the PhiC31 integrase system to insert the *ao* transgene into the 3rd chromosome (Groth et al. 2004), along with approximately 700 base pairs upstream and 300 base pairs downstream of the *ao* protein-coding sequence. (Since the *ao* promoter is not well defined, we chose to include the untranslated regions, but not coding sequences, of neighboring genes.) By crossing the Δ*ao* and 'rescue' *ao* strains, we obtained flies containing homozygous Δ*ao* mutations (on the 2nd chromosome) with two copies of the 'rescue' *ao* transgene (on the 3rd chromosome). The 'rescue' *ao* transgene is transcribed at only 20% of the level of the endogenous *ao* gene (Fig 2.3B). Despite its lower expression, the 'rescue' *ao* transgene is sufficient to fully suppress the maternal-effect lethality of Δ*ao* (Fig 2.3C), thereby demonstrating a causal association of the maternal-effect lethality we observed with loss of *ao*.

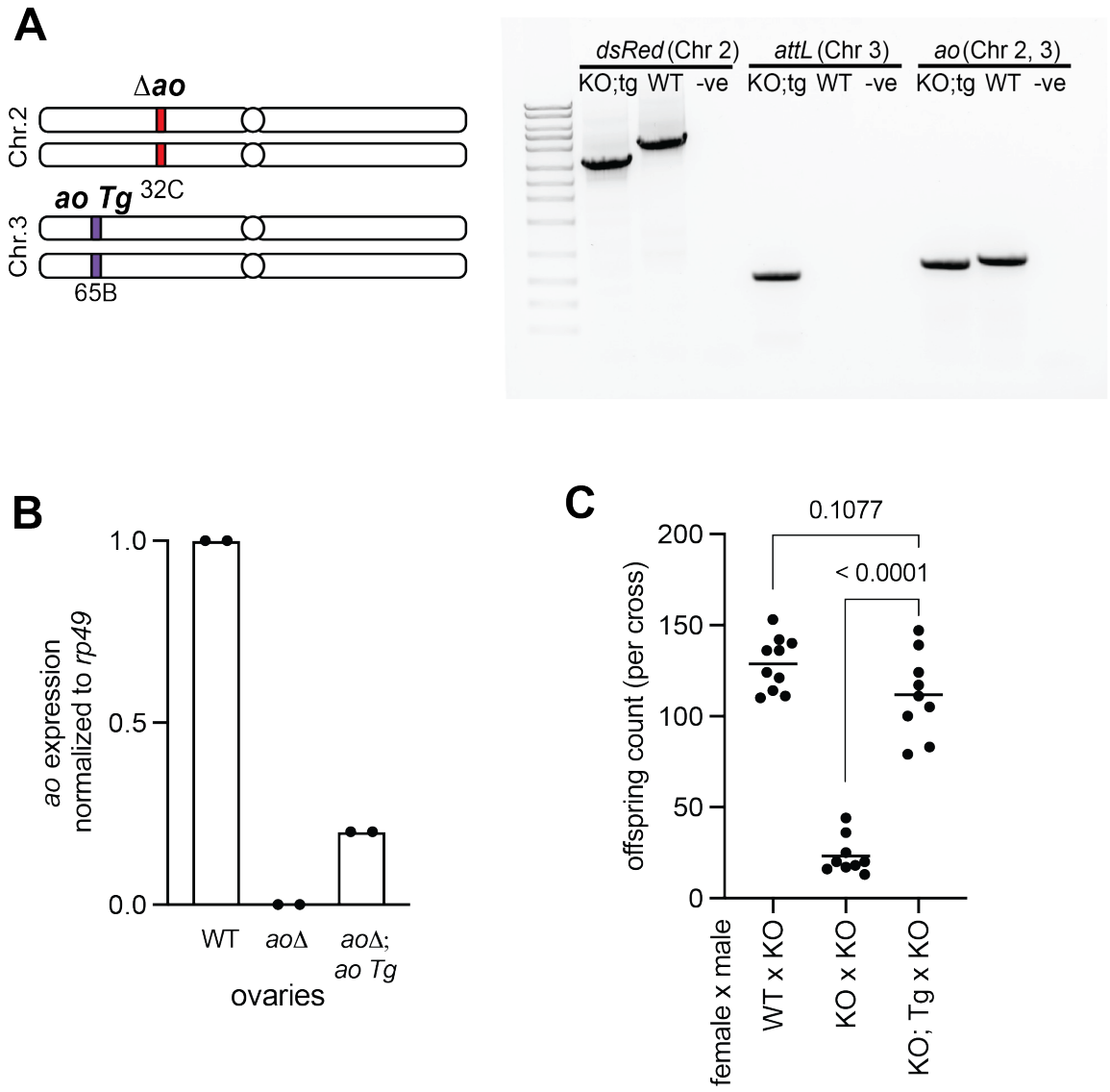

Figure 2.3: Generation and validation of the *ao*-transgene rescue construct. A) Schematic of the *ao*-transgene rescue construct. The *ao* coding sequence, as well as ~700bp upstream and ~300bp downstream, was inserted on the 3rd chromosome using the PhiC31 integrase system. The absence of the endogenous *ao* allele (and replacement with *dsRed*) on the 2nd chromosome, the presence of the *attL* site on the 3rd chromosome, as well as the presence of the *ao* allele on the 3rd chromosome (via transgene insertion) were confirmed with PCR. The expected wildtype and *dRed* band on the 2nd chromosome is 4139 bp and 3191 bp, respectively. Flies with a successful PhiC31 insertion have an *attL* site (expected band of 700bp). Δ*ao* flies carrying the *ao* transgene on the 3rd chromosome have a wildtype band (883 bp) for *ao,* the primers for which lie within the *ao* coding sequence. (See Fig 2.2 for a schematic of the *dsRed* and *ao* primers.) **B) Δ*ao* flies with 2 copies of the *ao* transgene have 20% *ao* expression relative to wildtype.** RT-qPCR on ovaries from virgin Δ*ao,* Δ*ao;tg,* and wildtype (isogenic *yw*) females. Each datapoint is a biological replicate of n=4 virgin ovaries. For each replicate, the median of the technical triplicate is shown. Gene expression has been normalized to *rp49.* **C) Fertility assay of Δ*ao* flies with the wildtype "rescue" *ao* transgene.** Crosses were set up and maintained at 29°C. All crosses were set up, flipped, and counted on the same days. KO is Δ*ao*, WT is the isogenic *yw* strain with wildtype *ao. p*-values are from two-tailed Mann-Whitney U tests.

Ao localizes to the histone gene cluster but does not affect histone transcript levels

Using a polyclonal antibody raised against Ao, a previous study observed localization of the Ao protein to the multigene array of histone genes on the 2nd chromosome in polytene chromosomes and mitotic chromosomes from larval neuroblasts (Berloco et al. 2001). Since this antibody is no longer available, we generated an *ao* strain tagged with the V5 epitope to visualize the Ao protein. We used CRISPR/Cas9 to insert the V5 tag at the 5' end of *ao* at the endogenous locus (Fig 2.4A). We confirmed that the *ao-V5* female flies have wildtype fertility at 29°C, indicating that the V5 tag does not interfere with the maternal-effect lethality-suppressing function of the Ao protein (Fig 2.4B). Given *ao*'s maternal-effect lethal phenotype, we assayed the localization of the Ao protein with a C-terminal V5 tag (Ao-V5) in ovaries using an antibody raised to the V5 epitope. We found that Ao-V5 colocalizes in the nucleus of ovaries with Multi sex combs (Mxc), a protein previously shown to localize specifically to the histone gene cluster (Fig 2.5; White et al. 2011). Ao-V5 and Mxc puncta colocalize in most but not all cells, which may indicate differences in the integrity of the histone locus body at different cell cycle stages.

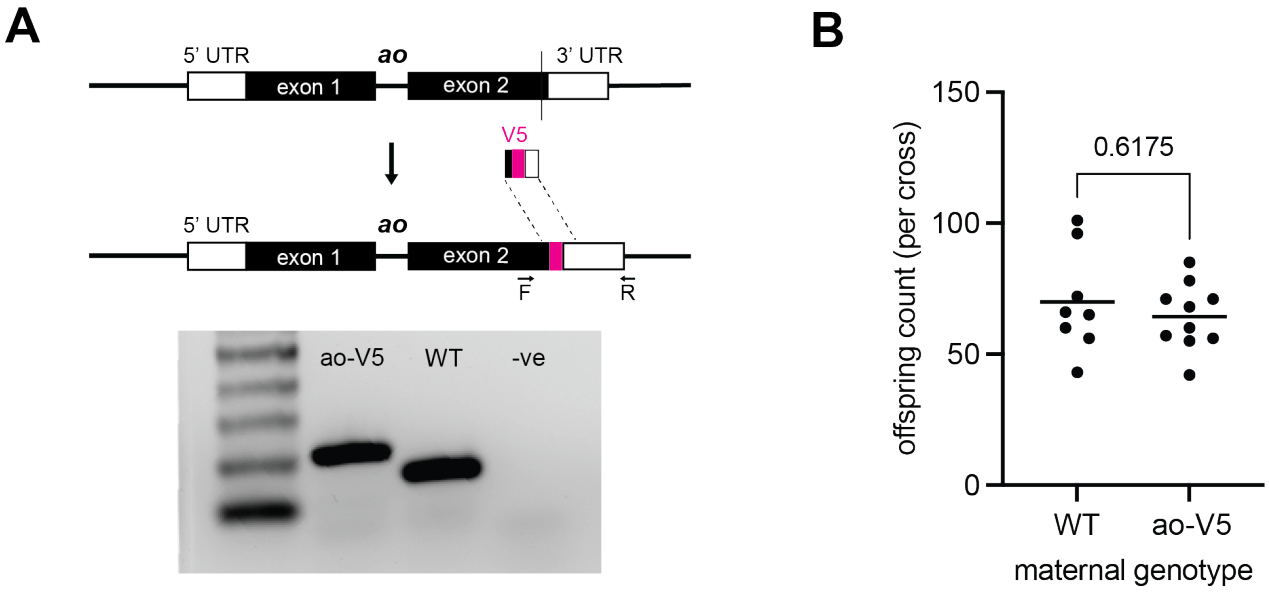

Figure 2.4: Generation and validation of the *ao-V5* flies. A) Schematic of the CRISPR/Cas9-mediated insertion of the V5 tag on the *ao* 5' end. The single-stranded oligo donor repair template contained the V5 tag (42 bp) and approximately 55 bp upstream and downstream of the insertion site. The V5-tag insertion was confirmed with PCR. The expected bands are 170 bp for wildtype (no V5 tag), and 212 bp with the V5 tag. **B) Fertility assay of *ao-V5* flies** mated to isogenic *yw* males with wildtype *ao.* Each point on the graph is the offspring count from a biological-replicate cross. Crosses were set up and maintained at 29°C. All crosses were set up, flipped, and counted on the same days. WT is the isogenic *yw* strain with wildtype *ao. p*-values are from two-tailed Mann-Whitney U tests.

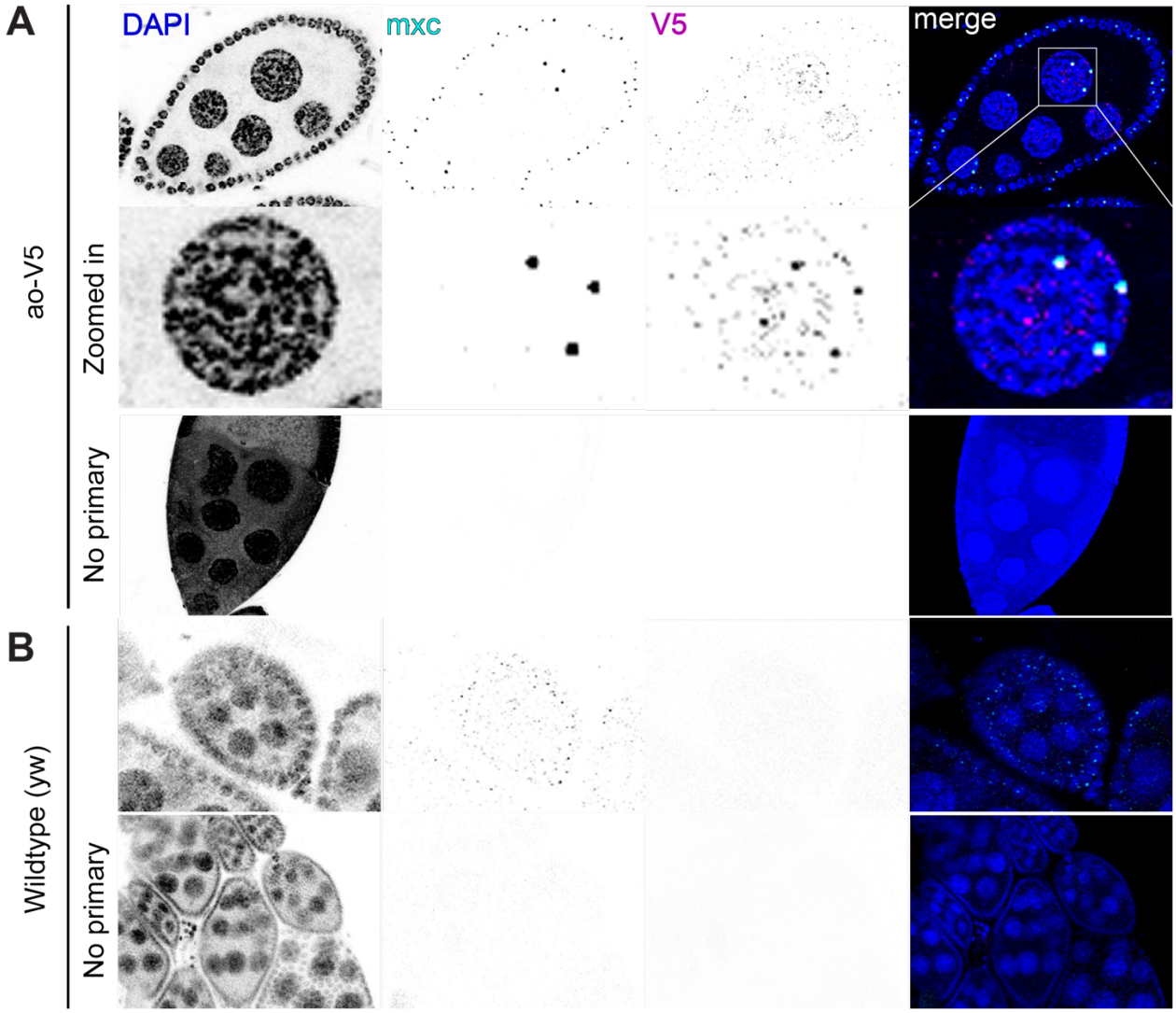

Figure 2.5: The Ao protein localizes to the histone gene cluster in ovaries. A) Immunofluorescence of *ao-V5* ovaries stained with the V5 and Mxc antibodies. The top row shows a single egg chamber containing polyploid nurse cells, and the second row is zoomed-in view of a single nucleus. The third row shows the control with no primary antibody. Nuclei are stained with DAPI. Mxc (Multi sex combs) localizes to the histone locus body, which assembles at the histone genes. The Mxc and V5 puncta colocalize, indicating that the Ao protein localizes to the histone gene array. The merged image is shown in color, with DAPI, Mxc, and V5 in blue, teal, and magenta, respectively. **B) Immunofluorescence of wildtype ovaries stained with the V5 and Mxc antibodies.** Wildtype flies are *yw* flies that are isogenic to Δ*ao* flies. The top row shows staining with both primary and secondary antibodies, and the bottom row is the control without the primary antibody. The same confocal settings were used to image all samples.

A remarkable finding from a previous study was the dramatic overexpression of core histone genes in *ao* mutants (Berloco et al. 2001). Based on Northern blotting analyses, it reported that unfertilized eggs from ao^1/ao^2 females had a 1.6-fold (for histone H4) to 11-fold (for histone H2A) increase in core histone transcripts relative to unfertilized eggs from wildtype Oregon-R females (Berloco et al. 2001). To quantify histone transcript levels in ovaries and unfertilized eggs from Δ*ao* virgin females, we performed quantitative reverse transcriptase PCR (RT-qPCR) for each of the four core histones and the linker histone. Surprisingly, we found no significant differences in core histone levels between Δ*ao* and isogenic-wildtype samples in both ovaries and unfertilized eggs (Fig 2.6A, B). We confirmed these results using a ribosomal-depletion RNA-seq experiment (Table 2.1, Appendix A).

Given the discrepancy between our Δ*ao*/Δ*ao* results and previous findings from ao^1/ao^2 flies, we quantified histone transcript levels in ao^1/ao^1 ovaries. (The ao^2 stock no longer exists.) Similar to our results from Δ*ao* ovaries, we found no significant differences in histone transcript levels (Fig 2.6C) in ovaries from ao^1/ao^1 and wildtype females. Thus, contrary to the previously published study, we conclude that *ao* does not affect histone gene expression at the steady-state RNA level.

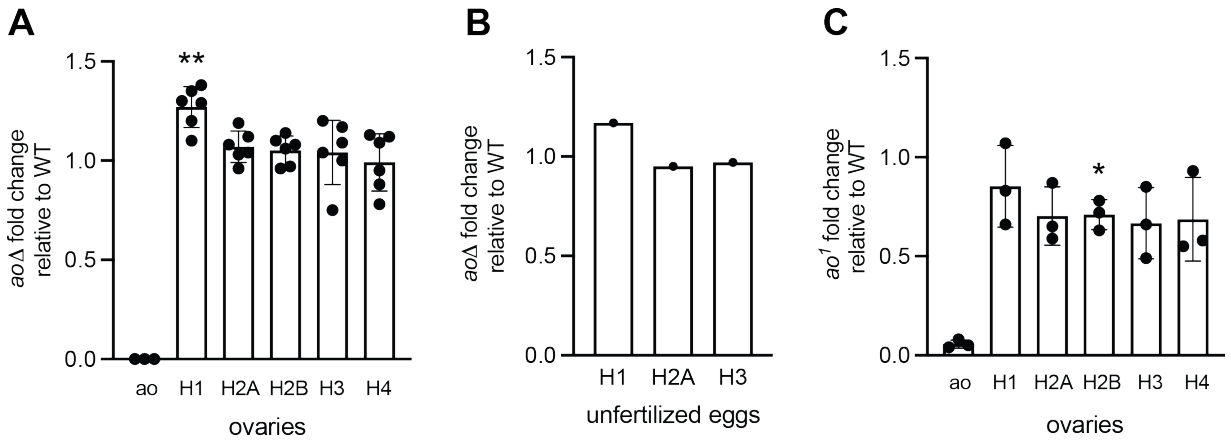

Figure 2.6: *ao* does not affect histone transcript levels. A) RT-qPCR on Δ*ao* ovaries. Each datapoint is a biological replicate of n=3-5 virgin ovaries. For each replicate, the median of the technical triplicate is shown. Gene expression has been normalized to *rp49.* **B) RT-qPCR on Δ*ao* unfertilized eggs.** RT-qPCR on 0-7-hour unfertilized eggs from Δ*ao* and isogenic *yw* 3-7-day-old virgin females. n=10 unfertilized eggs were used for each genotype. The median of the technical triplicate is shown. Gene expression has been normalized to *rp49.* **C) RT-qPCR on ao^1 ovaries.** Each datapoint is a biological replicate of n=3-5 virgin ovaries. For each replicate, the median of the technical triplicate is shown. Gene expression has been normalized to *rp49.*

Histone	Log_2(fold change) (Δ*ao*/WT)	Fold change	*p*-value (adjusted)
H1	0.03	1.02	0.73
H2A	-0.12	0.92	0.12
H2B	-0.14	0.91	0.13
H3	0	1	1
H4	0.06	1.04	0.59

Table 2.1: Core histone transcript levels from ribo-depletion RNA-seq analysis.

Genetic interactions between *ao* and histone genes

The previous finding that *ao* might encode a histone gene repressor motivated the hypothesis that *ao*-associated maternal-effect lethality could result from excess histones in eggs (Berloco et al. 2001). This hypothesis led to the prediction that *ao*-associated maternal-effect lethality might be rescued by a histone deficiency in *ao*-mutant mothers. Indeed, a heterozygous deletion of the histone locus in ao^1/ao^1 mutant females was shown to ameliorate their maternal-effect lethality (Berloco et al. 2001). Although we found no evidence of *ao* acting as a histone gene repressor, we nevertheless investigated whether a histone deletion could suppress the maternal-effect lethality of Δ*ao* females. We crossed Δ*ao* flies to a strain carrying a heterozygous deletion of the histone locus (BDSC 8670; Cook et al. 2012) to create Δ*ao*/Δ*ao* flies with half the copy number of wildtype histones (Fig 2.7A). We found that reducing histone copy number partially rescues the maternal-effect lethality of Δ*ao* females, just as previously reported for ao^1/ao^1 females (Fig 2.7A; Berloco et al. 2001).

We next assessed the relationship between histone gene copy number and *ao* expression using flies with a deletion of the entire histone locus on the 2nd chromosome and a transgenic histone gene cluster inserted on the 3rd chromosome (Fig 2.7B; McKay et al. 2015). The copy numbers on the transgenic histone cluster range from 112 to 12 copies per chromosome (wildtype flies have 100 copies of the histone gene cluster on each chromosome, for a total 200 copies per diploid fly). If *ao* were functioning as a histone transcriptional repressor, we hypothesized that

flies with lower histone gene copy numbers would have lower *ao* levels to enable higher histone gene expression, and vice versa. We quantified *ao* transcript levels in flies encoding 224, 200 (wildtype), 124, 100, and 24 copies of the histone gene cluster. Converse to this expectation, we found that flies encoding 24 copies of histone genes had a nearly 20% increase in *ao* transcript levels compared to flies encoding 100, 124, 200 (wildtype), or 224 copies of the histone gene cluster (Fig 2.7B).

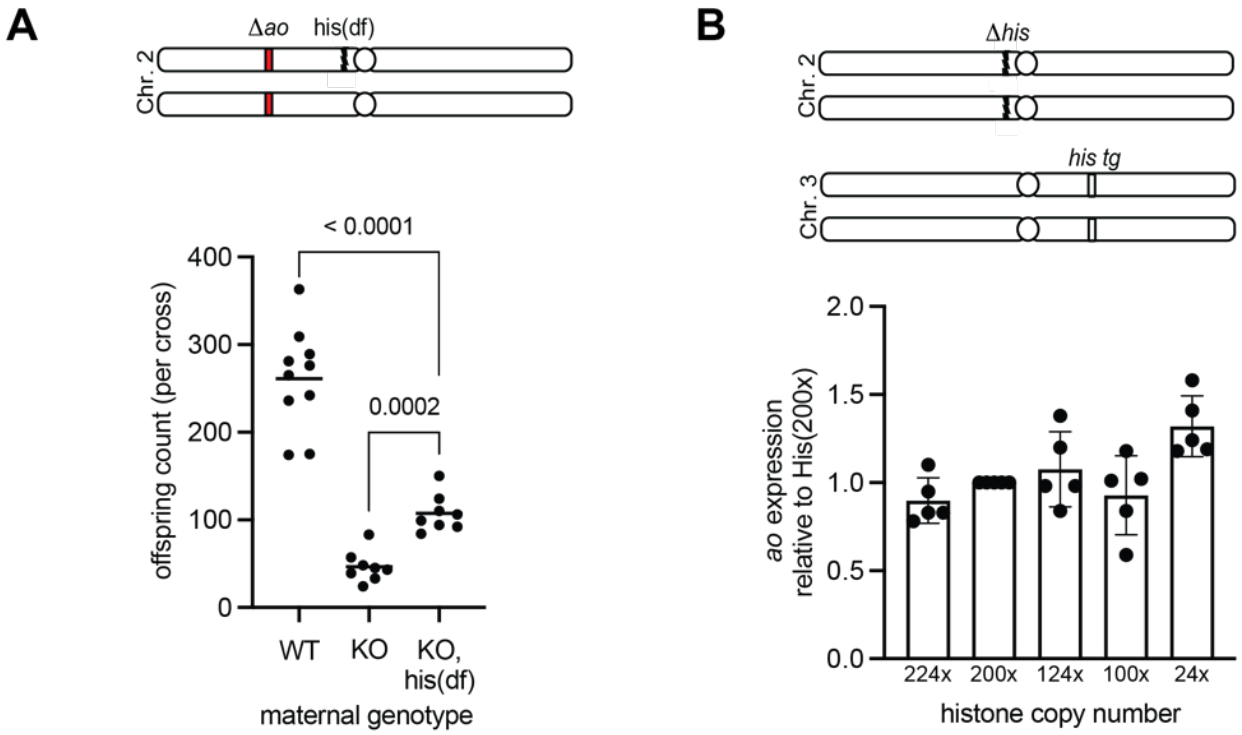

Figure 2.7: Relationship between *ao* and histone copy number. A) Histone deficiency ameliorates *ao*'s maternal-effect lethality. The histone deficiency flies have a deletion from cytological locus 39D3 to 39E2, corresponding to the histone gene array. Each point on the graph is the offspring count from a biological-replicate cross. All crosses were set up, flipped, and counted on the same days. KO is Δ*ao*, KO, his(df) is Δ*ao* with a heterozygous histone deficiency, and WT is the isogenic *yw* strain with wildtype *ao*. *p*-values are from two-tailed Mann-Whitney U tests. **B) *ao* expression increases in flies with 24x histone genes.** RT-qPCR on ovaries on flies with a deletion of the entire histone locus on the 2nd chromosome and a transgenic histone cluster on the 3rd chromosome. Each datapoint is a biological replicate of n=4 virgin ovaries. The mean of the biological replicate is shown for each replicate. Gene expression has been normalized to *rp49*.

Genetic interactions between *ao* and the Y-chromosome heterochromatin

Although *ao* mutant females produce fewer offspring than wildtype females, they are not skewed in their sex ratio. When crossed to males with attached X^Y chromosomes, however, *ao* mutant females produce an excess number of XX^Y female offspring relative to X0 male offspring (Sandler et al. 1968, Sandler 1970, Parry and Sandler 1974, Sandler 1977). This distortion of offspring sex ratio is attributed to the ability of specific regions of the X- and Y-heterochromatin to partially relieve *ao*-associated maternal effect lethality (Sandler 1970, Parry and Sandler 1974, Sandler 1977, Yedvobnick et al. 1980, Pimpinelli et al. 1985, Tomkiel et al. 1991). These special heterochromatic regions are called the AO heterochromatin, for their ability to rescue the *ao* lethality (Fig 2.8A; Pimpinelli et al. 1985).

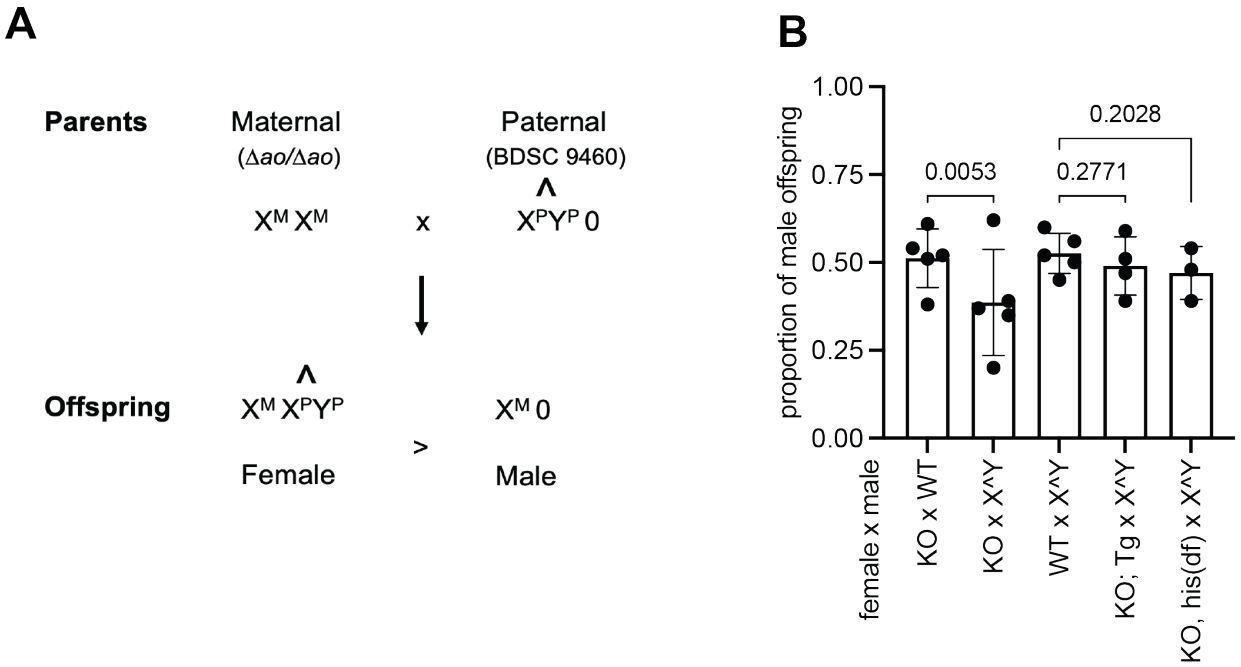

Figure 2.8: Excess Y chromosome rescues the Δ*ao* maternal-effect lethality. A) *ao* homozygous-mutant females produce an excess of female offspring when mated to males with an attached X^Y chromosome. Previous studies, starting with Sandler 1970, have noted that when mated to males with an attached X^Y chromosome, *ao* mutant females produce more female offspring compared to male offspring. This is attributed to the fact that XX^Y female offspring have more AO heterochromatin compared to X0 male offspring. (In *Drosophila*, the ratio of the X chromosomes to autosomes, rather than the presence of the Y chromosome, determines sex.) **B) Δ*ao* females produce an excess of female offspring when mated to males with an attached X^Y chromosome.** KO is Δ*ao*, KO;Tg is Δ*ao* with two copies of the *ao* transgene on the 3rd chromosome, KO, his(df) is Δ*ao* with a heterozygous histone deficiency, WT is the isogenic *yw* strain with wildtype *ao*, and X^Y is BDSC strain 9460. Crosses were set up and maintained at 25°C. *p*-values are from a 2x2 contingency table using the two-tailed Fisher's exact test.

We confirmed the interaction between the *ao* allele and AO heterochromatin on the Y chromosome using the Δ*ao* strain. Crosses between Δ*ao* females and wildtype males yielded nearly equal numbers of female (51%) and male (49%) offspring (Fig 2.7B). In contrast, crosses between Δ*ao* females and attached X^Y males (BDSC 9460) yielded a 61:39 female: male offspring ratio, which significantly deviated from the 50:50 expectation (p-value=0.0053). This skew in sex ratio was corrected in crosses between Δ*ao* females carrying two copies of the 3rd chromosome 'rescue' *ao* transgene and attached X^Y males (49% males). Similarly, crosses between Δ*ao* females carrying a histone deficiency and attached X^Y males also yielded nearly equal sex-ratios (47% males) (Fig 2.8B).

2.4: Discussion

Using our new Δ*ao* and *ao-V5* reagents, we recapitulated most of the previous genetic and cytological findings related to *ao*. These include the findings that *ao* encodes a protein that localizes to the histone gene cluster and plays a role in suppressing maternal-effect lethality, which can be rescued either by reduction of the histone gene copy number or by excess Y-heterochromatin. However, we did not find evidence supporting the model that *ao* encodes a transcriptional repressor of histones, or that transcriptional overexpression of histone genes results in *ao*'s maternal-effect lethality. Instead, our data suggest that a different molecular mechanism underlies *ao* function and its genetic interactions with the histone gene cluster and heterochromatin.

Pioneering genetic studies identified *ao* as a maternal-effect lethal gene whose maternal-effect lethality depended on heterochromatin content in zygotes (Sandler et al. 1968, Sandler 1970, Parry and Sandler 1974, Sandler 1977). A satisfying explanation for *ao*'s connection to heterochromatin emerged from a molecular study three decades after its initial characterization, which showed that the *ao*-encoded protein localized to the histone cluster and that its loss led to histone overexpression in unfertilized eggs from ao^1/ao^2 mothers (Berloco et al. 2001). The same study also demonstrated that a reduction in histone copy number ameliorated *ao*-associated maternal-effect lethality. These observations led to the model that histone overexpression in *ao/ao* mothers leads to high histone levels in eggs and zygotes, which results in the maternal-effect lethal phenotype. As a result of these findings, *ao* became a valuable tool for manipulating

histone gene expression in *Drosophila* (Chari et al. 2019), which cannot be accomplished by simply changing the histone gene copy number (McKay et al. 2015, Zhang et al. 2019).

However, these observations relied on reagents that have associated genetic background effects. Moreover, two important reagents – the ao^2 allele (Tomkiel et al. 1995) and the anti-Ao antibody (Berloco et al. 2001) – are no longer available. To fill this gap, we developed two novel tools: a precise CRISPR/Cas9-mediated deletion of the *ao* locus (and replacement with *dsRed*) and an *ao* allele tagged with the *V5* epitope at the endogenous locus. Using these reagents, we revisited key findings from the original *ao* studies. We confirmed *ao*-associated maternal-effect lethality and its amelioration via a reduction in histone copy number or excess Y-heterochromatin. We also confirmed the localization of the Ao protein to the histone cluster, both in early embryos and in ovaries. However, we found that *ao* is not a direct inhibitory transcription factor of histone genes; we observed no differences in histone RNA levels among Δ*ao*/Δ*ao*, ao^1/ao^1, and wildtype ovaries. Although *ao* likely has an indirect connection to histones and heterochromatin, as indicated by the rescue of maternal-effect lethality via reduction in histone copy number and excess heterochromatin, our work suggests that *ao* should not be used to directly manipulate histone levels.

Why is there a significant discrepancy in the histone overexpression phenotype between our Δ*ao* alleles and the previously characterized ao^1/ao^2 strain? Precise deletion null alleles (like Δ*ao*) can often differ in phenotype from presumed null alleles that leave part of the gene intact (like ao^1, which has a Doc transposon interrupting the first exon). This difference can result from a phenomenon called transcriptional adaptation (El-Brolosy et al. 2017), in which alleles that ablate mRNA transcription entirely can get compensated and, therefore, give less severe phenotypes than those that allow transcription of mutant mRNA (El-Brolosy et al. 2019).

However, in the case of *ao*, we suspect the explanation might stem from differences in genetic background among the strains. Like in Δ*ao*/Δ*ao* ovaries, we did not observe a histone overexpression phenotype in ao^1/ao^1 ovaries. Indeed, the overexpression of histone mRNAs was only observed in the ao^1/ao^2 trans-heterozygote (Berloco et al. 2001); ao^1/ao^1 flies had never been assessed for histone-transcript overexpression prior to our study. Unlike Δ*ao* and ao^1 alleles, ao^2 alleles could not be made homozygous (Tomkiel et al. 1995), indicating the presence of one or more recessive lethal mutations. Moreover, whereas a wildtype *ao* transgene rescues the

maternal-effect lethality of *ao*^{1} and Δ*ao* (Tomkiel et al. 1995, this study), a wildtype transgene rescue for histone overexpression in the *ao*^{1}/*ao*^{2} trans-heterozygote was never conducted (Berloco et al. 2001). These observations suggest that the genetic background of the *ao*^{2} allele conferred an additional phenotypic burden that is not directly related to Ao protein function. Another possibility is that the *P*-element insertion in the 5'UTR of *ao* in the *ao*^{2} strain inadvertently affected the expression of *ATPsynG*, a gene that encodes a mitochondrial ATP synthase subunit and is located upstream of *ao.* Unfortunately, since the *ao*^{2} strain is no longer available, we cannot identify the nature of these additional background effects or how they might relate to histone overexpression.

Our findings that Ao is not a transcriptional repressor of histone genes are also consistent with the fact that Ao's plant and mammalian orthologs belong to the DET1 family of E3 ubiquitin ligases (Berloco et al. 2001). We explore this possibility further in Chapter 3.

2.5: Materials and methods

Generation of the Δ*ao* line

We used CRISPR/Cas9 to create an *ao* knockout line. To facilitate the screening of transgenic flies, we replaced the *ao* allele with *dsRed* under the eye-specific promoter *3xP3.* We chose guide RNAs with the best efficiency score and no predicted off-targets (https://www.flyrnai.org/crispr/). We cloned guide RNAs (AGCCGGGTTCTTCTTCCGAT and AGTAATGTCTTTATTTACAA) targeting the 5' and 3' ends of the *ao* gene into pCFD4 U6:1_U6:3tandemgRNAs (Port et al. 2014; Addgene plasmid #49411). The repair template sequence, including homology arms spanning approximately 1kb upstream and downstream of the *ao* coding sequence, was cloned into pDsRed-attP (Gratz et al. 2014; Addgene plasmid #51019). To prevent guide RNAs from targeting PAM sites, we mutated the PAM sites using the Q5 Site-Directed Mutagenesis Kit (New England Biolabs).

BestGene Inc. (Chino Hills, CA) prepared and co-injected the plasmids into BDSC 51323 embryos, which express *vas-Cas9* on the X chromosome. Following injection, BestGene Inc. crossed the injected flies to a *yw* strain to isolate transformants, crossed out the *Cas9* gene, and then balanced the 2nd chromosome over *CyO.* We verified the absence of *ao* and the presence of

dsRed with PCR and Sanger sequencing (see Table 2.2 for primer sequences). We extracted genomic DNA with the DNeasy Blood & Tissue Kit (Qiagen) according to the manufacturer's protocol for insect tissue. We performed PCR using the Platinum PCR SuperMix High Fidelity (Invitrogen). The penetrance of the *CyO* phenotype decreased with temperature, which made it difficult to distinguish between homozygote-null and heterozygous flies. We, therefore, rebalanced the Δ*ao* allele over *CyO-gfp* marked with *mini-white*, which enabled us to screen for homozygous flies based on eye pigment color. To allow for *mini-white* visualization, the *CyO-gfp* strain carries *yw* on the X chromosome. We crossed the *yw* strain from BestGene with our *yw; CyO-gfp* strain to obtain a near-isogenic strain to our Δ*ao* strain and used this strain as the wildtype control for all experiments.

To obtain an Δ*ao* strain with a heterozygous histone deletion, we crossed our Δ*ao* flies into the BDSC 8670 strain (Cook et al. 2012), which has a heterozygous deletion on the 2nd chromosome corresponding to the histone gene array (chromosomal locus 39D3 to 39E2). Both the *ao* allele and histone genes are located on the left arm of the 2nd chromosome, so after obtaining a female fly heterozygous for both Δ*ao* and histone deficiency, we relied on recombination to obtain a fly homozygous for Δ*ao* and heterozygous for histone deficiency. We used this fly to make the Δ*ao, his(df)* stock. The histone deletion is not marked, so we used PCR using the Phusion High-Fidelity DNA polymerase (New England Biolabs) to determine its presence in the founder fly (see Table 2.2 for primer sequences).

Generation of the *ao*-transgene rescue line

We used the PhiC31 integrase system to create the "rescue" line with wildtype *ao*. We cloned the *ao* coding sequence with its endogenous promoter into the pattB plasmid, which contains an *attB* site and *mini-white* marker (Bischof et al. 2013; DGRC stock 1420). BestGene Inc. prepared and injected the plasmid into BDSC 9750 embryos, which have the VK33 *attP* landing site on the 3rd chromosome (Venken et al. 2006). BestGene Inc. confirmed successful integration with PCR to verify the presence of the recombined *attL* site and absence of the original *attP* site (see Table 2.2 for primer sequences), then crossed out the gene encoding the PhiC31 integrase and balanced the 3rd chromosome over *TM6B*.

Generation of the V5-tagged *ao* line

We used CRISPR/Cas9 to tag *ao* at its N- and C-termini with a V5 epitope. We chose guide RNAs closest to the start and stop codons of *ao* with no off-targets (http://targetfinder.flycrispr.neuro.brown.edu/). We cloned guide RNAs (targeting the start codon of *ao*: CGATTGTAGGCGCTTCTTGT; targeting the stop codon of *ao*: GTATAACCACAGCACAATAG) into pCFD5 (Port and Bullock 2016; Addgene plasmid #73914). We designed single-stranded oligo donor (ssODN) repair templates containing the V5 tag (42 bp) and approximately 55 bp up- and downstream of the insertion site. The ssODNs had mutated PAM sites to prevent re-targeting.

We sent midi-prepped pCFD5 plasmids containing the guide RNAs and lyophilized ssODNs to GenetiVision Inc. (Houston, TX) for injection into embryos expressing *nanos-Cas9.* We screened for transformants using a PCR strategy, with primers that annealed just upstream and downstream of the insertion site (see Table 2.2 for primer sequences). We tested for insertion of the V5 tag by the presence of a 42 bp shift in band size. Finally, we confirmed the successful insertion of the intact V5 tag by Sanger sequencing.

Fly husbandry and fertility assays

Flies were maintained on the benchtop at room temperature on corn syrup/soy media made in-house at Fred Hutch Cancer Center (Seattle, WA) or purchased from Archon Scientific (Durham, NC). To conduct fertility assays, we used 1-to-5-day-old males and virgin females raised at room temperature. We paired 4 virgin females with 2 males in a vial with corn syrup/soy media and allowed them to mate for 3 days (for X^Y assays) or 1 week (for all other assays). To prevent larval overcrowding in the vials, we flipped the parents to new vials after 3 days and discarded the parents from the new vials 4 days later. The crosses were set up and maintained at 18°C, 25°C, or 29°C, as noted for each experiment. We counted the adult offspring (F1) to exhaustion.

We excluded crosses with no larvae in one or both vials from statistical analyses. Because non-genetic factors, including variation in food and ambient humidity, influence fly fertility, we only compared data among the crosses set up on the same day. We used GraphPad Prism version 10.1.1 for macOS (GraphPad Software) to plot the data and conduct statistical analyses. To compare the offspring count between the two datasets, we performed two-tailed Mann-Whitney

U tests and reported exact *p*-values. To compare the observed offspring genotype to the theoretical Mendelian offspring genotype in Fig 2.2C, we used a one-sample proportion test (http://www2.psych.purdue.edu/~gfrancis/calculators/proportion_test_one_sample.shtml). To compare the results of X^Y crosses in Fig 2.8B, we analyzed a 2x2 contingency table using a two-tailed Fisher's exact test on the GraphPad website (https://www.graphpad.com/quickcalcs/contingency1/).

Immunofluorescence

Ovaries were dissected in PBS, then fixed with 1:1 paraPBT: heptane (paraPBT = 4% paraformaldehyde in PBS + 0.1% Triton X-100) in an Eppendorf tube for 10 minutes at room temperature. Following three 5-minute washes in PBST (PBS + 0.1% Triton X-100), we blocked the ovaries in PBST with 3% BSA for 30 minutes at room temperature. We incubated the ovaries in primary antibodies overnight at 4°C. We used a guinea pig anti-Mxc (gift from Robert Duronio) at [1:5000] and the V5 Tag monoclonal antibody (Thermo R960-25) at [1:250]. After three 5-minute washes in PBST, the samples were incubated with secondary antibodies in PBST for 2 hours at room temperature. We used the goat anti-mouse IgG Alexa Fluor 568 (Thermo A-11031) and goat anti-guinea pig IgG Alexa Fluor 488 (Thermo A-11073), both at [1:2000]. Hoechst stain (Invitrogen) was added to the samples in the last 30 minutes of the secondary-antibody incubation. After three 5-minute washes with PBST, the ovaries were mounted onto slides with 20µL of SlowFade Gold Antifade Mountant with DAPI (Invitrogen), then coverslips were added and sealed with nail polish.

RNA extraction and RT-qPCR

We dissected ovaries from 4-day-old virgin females in PBS. To collect unfertilized eggs, we let 3-to-7-day-old virgin females lay on grape plates for 7 hours. We transferred 4 pairs of ovaries or 10 unfertilized eggs to an Eppendorf tube and homogenized the tissue in 20µL of TRIzol (Invitrogen) with a disposable pestle and electric homogenizer. The samples were stored at -80°C in 100µL of TRIzol until ready to be processed. We incubated the thawed samples in 1mL of TRIzol for 5 minutes, then centrifuged at 13,000rpm for 10 minutes at 4°C to separate the supernatant. We extracted the supernatant with chloroform and then extracted the soluble phase with isopropanol. After a wash in 70% ethanol, the RNA pellet was resuspended in RNAse-free water. The samples were treated with DNAse I (Zymo Research) and then purified with the RNA

Clean & Concentrator-5 kit (Zymo Research). We quantified the purified samples with the Qubit RNA Broad Range Assay Kit (Invitrogen), then synthesized cDNA using the SuperScript III First-Strand Synthesis System with random hexamers (Invitrogen).

To perform RT-qPCR, we used the PowerUp SYBR Green Master Mix for qPCR (Applied Biosystems) with approximately 10ng of cDNA per reaction. We used the QuantStudio 3 Real-Time PCR System (Applied Biosystems) to run the RT-qPCR experiment (see Table 2.2 for primer sequences). For each primer pair, we ran each sample in technical triplicates and used the median value for analysis. We normalized gene expression to the reference gene *rp49* and calculated fold change using the $2^{-\Delta\Delta Ct}$ method.

Purpose	ID	Primer sequence (5' to 3')
ao KO validation	F1 (RT_070_F)	AACATCTCTGTTTCGTCGCACACTGAATAGG
ao KO validation	R1 (RT071_R)	TTGCGTCAAATTGATAAGCACACAGCCTCTCTTTGC
ao KO validation	F2 (RT068_F)	CAGGACACCATACTCAAGAGCAGGATCTTTGAACG
ao KO validation	R2 (RT069_R)	TGTAGTCATTGAATTGCAGTAAGATTTGCAGCAGGTTGAC
phiC31 validation	attP.FWD	TGCCCCAACTGGGGTAACCTTTG
phiC31 validation	attL.FWD	GGGCGTGCCCTTGAGTTCTCTC
phiC31 validation	65B2.REV	AACGCTTTGCTTTCTCGCTG
his(df) validation	his(df) FWD Set 14	CAA CCA AAC TCT ATT CCG ACA TT
his(df) validation	his(df) REV Set 14	GCT ACA GCT AAC AAC TGT ATG TG
his(df) validation	his(df) FWD Set 15	TCC GAC ATT AAA GAT GTC GTA TGG
his(df) validation	his(df) REV Set 15	AGA GCG AAG AGC GCT ACA
V5-tag validation	RT138_V5C_2F	ACGTCTACCACGTGCACTTG
V5-tag validation	RT139_V5C_2R	GACATTACTGAAAAGGTAAAACGAGATATTTTAGTATCAC
RT-qPCR	D. mel H3 FWD Set 2	TGC CCA AAG ACA TCC AGT TAG
RT-qPCR	D. mel H3 REV Set 2	GAG TAC GCT AGC GCT TTA TCT G
RT-qPCR	D. mel H4 FWD Set 5	GAAGCGCATATCTGGACTCATA
RT-qPCR	D. mel H4 REV Set 5	TCTTCCTCTTGGCGTGTTC
RT-qPCR	D. mel H2A FWD Set 3	CAA AGT GAA GGG AAA GGC AAA G
RT-qPCR	D. mel H2A REV Set 3	CCG GAG CAA ACG GTG AAT A
RT-qPCR	D. mel H2B FWD Set 1	GTC GAA GGC GAT GAG CAT AAT
RT-qPCR	D. mel H2B REV Set 1	CGC TTG TTG TAG TGA GCT AGA C
RT-qPCR	D. mel H1 FWD Set 4	AGG GTG CAT CTG GAT CTT TC
RT-qPCR	D. mel H1 REV Set 4	TAG AGG CTA CCT TCT TGC TTT G
RT-qPCR	D. mel ao FWD Set 3	TAG GCG TCG TCA CAG ATA GA
RT-qPCR	D. mel ao REV Set 3	CTT ACC GTC ATT CAC CCA ATA GA
RT-qPCR	AAD0394_Rp49mel_F	ATG ACC ATC CGC CCA GCA TAC
RT-qPCR	AAD0395_Rp49mel_R	GTT CTG CAT GAG CAG GAC CTC C

Table 2.1: Primer sequences used in Chapter 2.

2.6: Acknowledgements

I thank Casey Schmidt (Rieder lab, Emory University) for sharing the *ao-V5* flies she generated, Sierra Simmerman (Malik lab, Fred Hutch) for performing the cytology experiments and for assistance with fertility assays and *Drosophila* husbandry, and Robert Duronio for the Mxc antibody.

Chapter 3: Ao as an E3 ubiquitin ligase

3.1: Abstract

Ao belongs to the DET1 family of E3 ubiquitin ligases. Here, we explore the possibility that the *Drosophila* Ao mutant phenotype might also stem from its putative E3 ubiquitin ligase activity. To look for Ao's direct binding partners and putative targets, we performed two assays. We first did a pull-down experiment with HA-tagged *ao* ovaries to identify Ao's interactors. We also performed a yeast two-hybrid assay using the Ao protein as bait to identify any *Drosophila* proteins that serve as binding partners. We also performed tandem mass tag (TMT) mass spectrometry with Δ*ao* and wildtype ovaries to identify potential proteins whose levels might depend on the Ao protein. Based on the results, we hypothesize that Ao might act as an E3 ligase to regulate the *Drosophila* separase (Three rows) by targeting the *Drosophila* securin (Pimples). We also consider the possibility that Ao might control levels or ubiquitination of other proteins, including histones.

3.2: Introduction

Eukaryotes have multiple E3 ligases, which facilitate the transfer of ubiquitin from an E2 ubiquitin-conjugating enzyme to specific substrates. Ubiquitination marks the target protein for degradation by the 26S proteasome or alters the function of the target protein (Jackson and Xiong 2009). The largest known class of ubiquitin ligases is the Cullin-RING ligase family (Petroski and Deshaies 2005). A Cullin-RING E3 ubiquitin ligase complex comprises: 1) a RING (Really Interesting New Gene) finger protein, which catalyzes the transfer of ubiquitin from an E2 ubiquitin-conjugating enzyme to the substrate, 2) a cullin, a scaffold protein that recruits the RING finger protein, 3) a substrate-recognition subunit that binds specific regions, or degrons, on the substrate, and 4) a linker, or adaptor protein, which bridges the substrate-recognition unit and the cullin (Petroski and Deshaies 2005).

Cullin proteins are the scaffold of the Cullin-RING complex. There are multiple cullins – *Drosophila* and humans have six, whereas *Arabidopsis* has nine – each associated with specific adaptor proteins and substrate-recognition subunits (Jackson and Xiong 2009). Cullin-4A (CUL4A) interacts with the adaptor protein DNA-damage-binding-protein-1 (DDB1), which in

turn binds to the substrate-recognition unit (Petroski and Deshaies 2005). Based on protein structure and domain architecture, DET1 (the ortholog of *Drosophila* Ao) is the substrate-recognition subunit of the COP1-CUL4A-RING E3 ubiquitin ligase complex (L. Aravind, personal communication). Studies have also characterized DET1 as a linker component of this E3 ubiquitin ligase complex that acts to enhance E2 activity (Yanagawa et al. 2004, Pick et al. 2007).

det1 was first identified in *Arabidopsis thaliana* as a negative regulator of light-mediated growth in seedlings (Chory et al. 1989). *det1* mutant plants exhibit light-dependent phenotypes, including in leaf and chloroplast development, as well as accumulation of anthocyanin and mRNAs for light-regulated nuclear and chloroplast genes even in the absence of light (Chory et al. 1989, Chory and Peto 1990, Pepper et al. 1994). The DET1 protein was later shown to associate with DDB1 and COP10 to enhance E2 activity (Schroeder et al. 2002, Yanagawa et al. 2004), and with CUL4 to assemble an E3 ligase (Bernhardt et al. 2006). The human ortholog, *hDet1*, was subsequently also identified as a component of the COP1 CUL4A-RING E3 ligase that targets c-Jun, a proto-oncogenic transcription factor (Wertz et al. 2004, Pick et al. 2007). Subsequent studies have identified additional targets of this complex, including the transcription factor c/EBPβ, which regulates pro-inflammatory genes in microglia and is upregulated in patients with Alzheimer's disease (Ndoja et al. 2020).

Intriguingly, both plant and human DET1 have been implicated in chromatin remodeling. In tomatoes and *Arabidopsis*, DET1 binds to nonacetylated, C-terminal H2B tails in the nucleosome (Benvenuto et al. 2002). In *Arabidopsis*, DET1 regulates H2B monoubiquitination by degrading a deubiquitination module in a light-dependent context (Nassrallah et al. 2018). Although there is no direct evidence of human hDET1 interacting with histones, the CUL4-DDB-ROC1 ubiquitin ligase complex does polyubiquitinate H3 and H4 in HeLa cells (Wang et al. 2006). The same study showed that CUL4-DDB-ROC1 ubiquitylates all four core histones at multiple lysine residues *in vitro* (Wang et al. 2006). Additionally, the DDB1-CUL4A^{DDB2} ubiquitin ligase targets H2A for monoubiquitination in human cell lines (Kapetanaki et al. 2006).

Here, we hypothesized that *Drosophila* Ao, like its plant and mammalian orthologs, functions as a subunit of the COP1 Cul4A-RING E3 ubiquitin ligase complex. We considered the possibility that Ao, like its plant and human counterparts, also regulates histones post-transcriptionally, but

also considered that Ao may have additional targets. We took three approaches to determine Ao's target(s): 1) pull-down mass spectrometry using HA-tagged *ao* ovaries to determine Ao's interactors *in vivo* (to detect proteins that interact directly with Ao, as well as those that belong to complexes in which another proteins binds to Ao), 2) a yeast two-hybrid assay to determine Ao's direct interactors, and 2) TMT mass spectrometry with Δ*ao* and wildtype ovaries to investigate potential targets of Ao's E3 ligase.

3.3: Results

Ao has many potential binding partners

We took two orthogonal approaches to look for Ao's potential binding partners. We first performed a pull-down mass spectrometry (pull-down MS) experiment on flies with overexpression of HA epitope-tagged *ao* using the GAL4/UAS system. The GAL4/UAS system in *Drosophila* allows for targeted gene expression in specific tissues (Brand and Perrimon 1993, reviewed in Duffy 2002). This system comprises two parts: the tissue-specific GAL4 driver line, which encodes the yeast transcription factor GAL4, and the upstream-activating sequence (UAS) responder line, which encodes the gene of interest under the control of a UAS site. We crossed the UAS-*ao-HA* line (FlyORF F001850; Bischof et al. 2013), which encodes *ao* that is epitope-tagged with a triple-HA tag under the control of UAS promoter, to the maternal triple driver (MTD)-GAL4 line (BDSC 31777), which carries three GAL4 constructs with germline and maternal-tissue expression (Grieder et al. 2000, Mazzalupo and Cooley 2006). We dissected ovaries from the F1 offspring of this cross, which overexpress the HA-tagged *ao.* To control for nonspecific protein binding in offspring from the MTD-GAL4 line, we also crossed the MTD-GAL4 driver to a UAS-*GFP-nls* responder line (BDSC 4776), which encodes nuclear localization signal (*nls*)-tagged green fluorescent protein (*GFP*) under the control of the UAS promoter. We used the F1 from this cross as the control for the pull-down MS experiment.

The pull-down identified 1,468 proteins, 107 of which were detected in significantly greater quantities in the *ao-HA* samples relative to the *GFP-nls* samples ($\log_2$ fold change > 1.0, p-value < 0.05). Of these, 17 proteins were identified as significant based on a false discovery rate (FDR) < 0.10. We have not yet explored the biological significance of these proteins in detail, but they

include several with chromatin-related functions, including CG7379, Mcm6, and PARP1, as well as Spd-2 and Cp110, which are essential for centrosome integrity (Fig 3.1, Table 3.1). Additionally, CG12608 and Srp68 have ribosomal functions (Fig 3.1, Table 3.1).

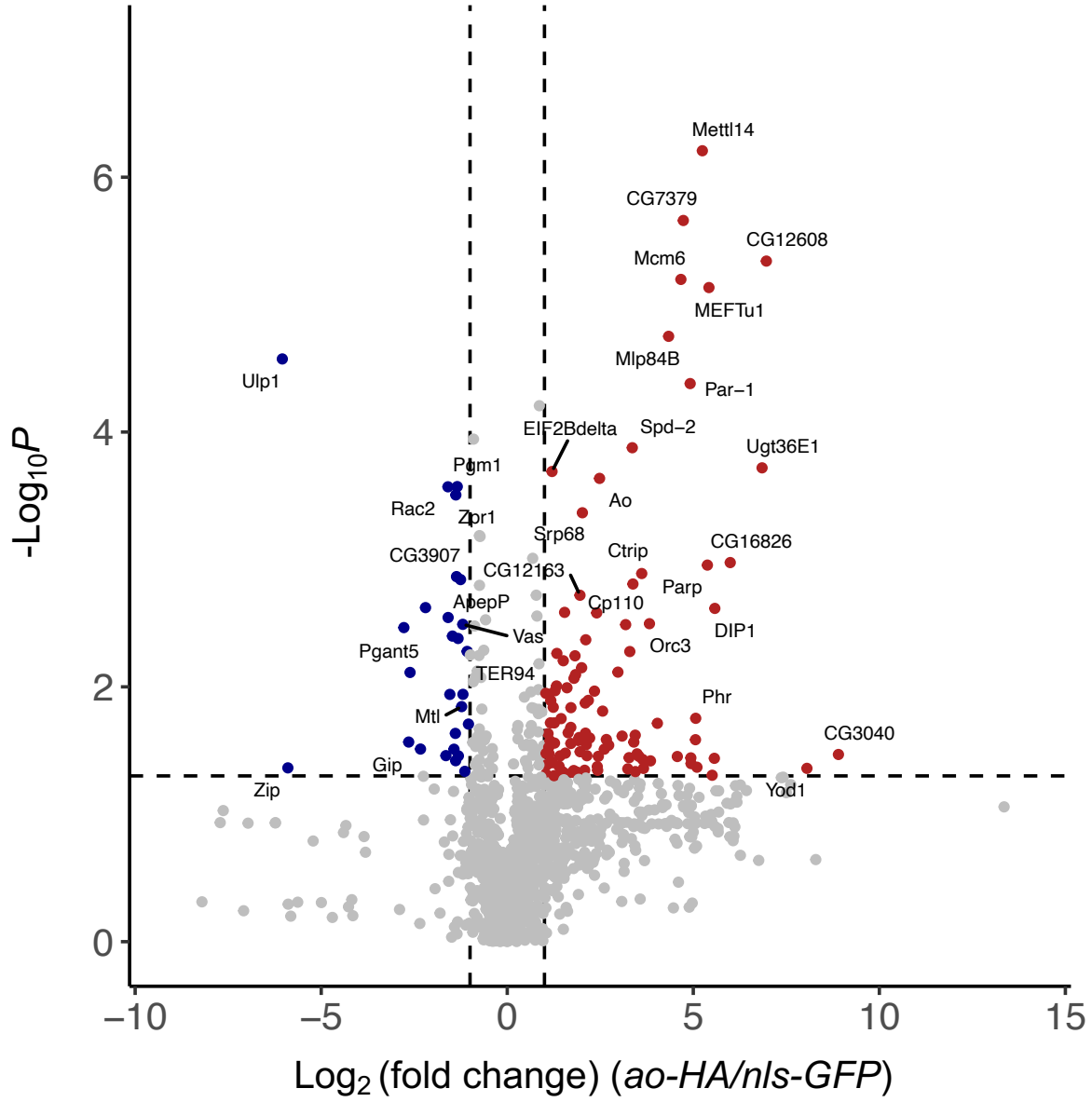

Figure 3.1: Proteins identified in pull-down mass spectrometry using *ao-HA* ovaries. 1,468 total proteins were identified. Proteins in red have $\log_2$(fold change) > 1.0 and *p*-value < 0.05; 17 of these have FDR < 0.10. Proteins in blue have $\log_2$(fold change) < -1.0 and *p*-value < 0.05.

Protein	Fold change *(ao-HA/nls-GFP)*	*p*-value	FDR
Mettl14	37.88	6.20E-07	0.001
CG7379	26.58	2.19E-06	0.002
CG12608	124.85	4.55E-06	0.002
Mcm6	25.41	6.34E-06	0.002
mEFTu1	42.83	7.35E-06	0.002
Mlp84B	20.21	1.77E-05	0.004
Par-1	30.20	4.17E-05	0.008
Spd-2	10.27	1.33E-04	0.018
eIF2Bdelta	2.30	2.04E-04	0.023
Ugt36E1	115.23	1.91E-04	0.023
Ao	5.58	2.31E-04	0.024
Srp68	4.05	4.30E-04	0.035
CG16826	63.69	1.06E-03	0.071
Parp	41.61	1.11E-03	0.071
Ctrip	12.25	1.29E-03	0.079
Cp110	10.39	1.56E-03	0.084
CG12163	3.88	1.91E-03	0.093

Table 3.1: Proteins identified in pull-down MS with $\log_2$(fold change) > 1.0 and FDR < 0.10.

As an orthogonal approach to the *ao-HA* pull-down MS, we looked for Ao's interactors using the yeast two-hybrid assay (Fields and Song 1989). In the yeast two-hybrid assay, the protein of interest (bait) is fused to the DNA binding domain of a transcription factor such as GAL4. The candidate interacting proteins (prey) are individually fused to the activation domain of the same transcription factor. Bait-and-prey interaction activates the reporter genes downstream of the transcription factor. The yeast cells are selected for the presence of the reporter gene and the positive clones are sequenced. With the help of Hybrigenics Services (Évry-Courcouronnes, France), we performed yeast two-hybrid assays with the LexA and GAL4 transcription factors, using a cDNA library derived from *D. melanogaster* ovaries. We performed both the LexA and GAL4 assays to obtain both a wide spectrum and maximum sensitivity in detecting potential interactors; LexA is a more efficient but less sensitive system than GAL4.

The LexA screen revealed 12 positive clones out of the 92 million tested interactions. (The bait and prey proteins are protein fragments, not full-length proteins.) Two proteins were identified from the analysis as potential interactors of Ao: CG14478 and His4r (Table 3.2). A subsequent

screen with GAL4, which identified 21 positive clones out of the 111 million tested interactions, additionally identified Abl as an additional interactor (Table 3.2). A final screen using an inducible GAL4 vector, which revealed 94 positive clones out of the 88.8 million tested interactions, identified Nod as the fourth potential interactor of Ao (Table 3.2). However, only one of these four hits (CG14478) was identified as a good-confidence hit in the two-hybrid assay. None of these four proteins were detected as significant hits in the pull-down MS with the *ao-HA* ovaries.

Protein	Screen	Score	Vector
CG14478	LexA	C	N-bait-LexA-C
	GAL4	D	N-GAL4-bait-C
His4r	LexA	E	N-bait-LexA-C
	GAL4	E	N-GAL4-bait-C
Abl	GAL4	D	N-GAL4-bait-C
Nod	GAL4, inducible	D	N-GAL4-bait-C, inducible

Table 3.2: Proteins identified in the yeast two-hybrid assay. A score of C indicates good confidence in the interaction; D indicates moderate confidence in the interaction; E indicates interactions involving highly connected prey domains, warning of non-specific interaction.

Ao has several (potential) targets

To determine Ao's targets more broadly (*i.e.,* to cast a net to include proteins whose levels depend on Ao, but do not interact directly with Ao), we performed a TMT mass spectrometry (TMT MS) experiment on Δ*ao* and isogenic-wildtype ovaries from virgin females. TMT MS is a quantitative approach to measure differential protein abundance between different samples. First, peptides from protein samples are labeled with tags. The tags are isobaric, with the same nominal mass, but differ in their isotopic compositions. The samples are then multiplexed through the mass spectrometer, where they are ionized and generate signals corresponding to their masses. In the second MS spectrum, the TMT tags on the peptides produce reporter ions that indicate the relative abundance of the peptide in the sample (Pappireddi et al. 2019).

The TMT MS experiment identified a total of 6,691 proteins (Fig 3.2). Of these, 49 proteins were significantly more abundant in Δ*ao* ovaries ($\log_2$ fold change > 1.0, p-value < 0.05). However,

only four proteins out of the 49 met the threshold of significance with a false discovery rate (FDR) < 0.05 (Table 3.3). Additionally, 56 proteins were significantly less abundant in Δ*ao* ovaries (log_2 fold change < -1.0, p-value < 0.05), of which seven proteins met the statistical threshold of FDR < 0.05 (Table 3.4).

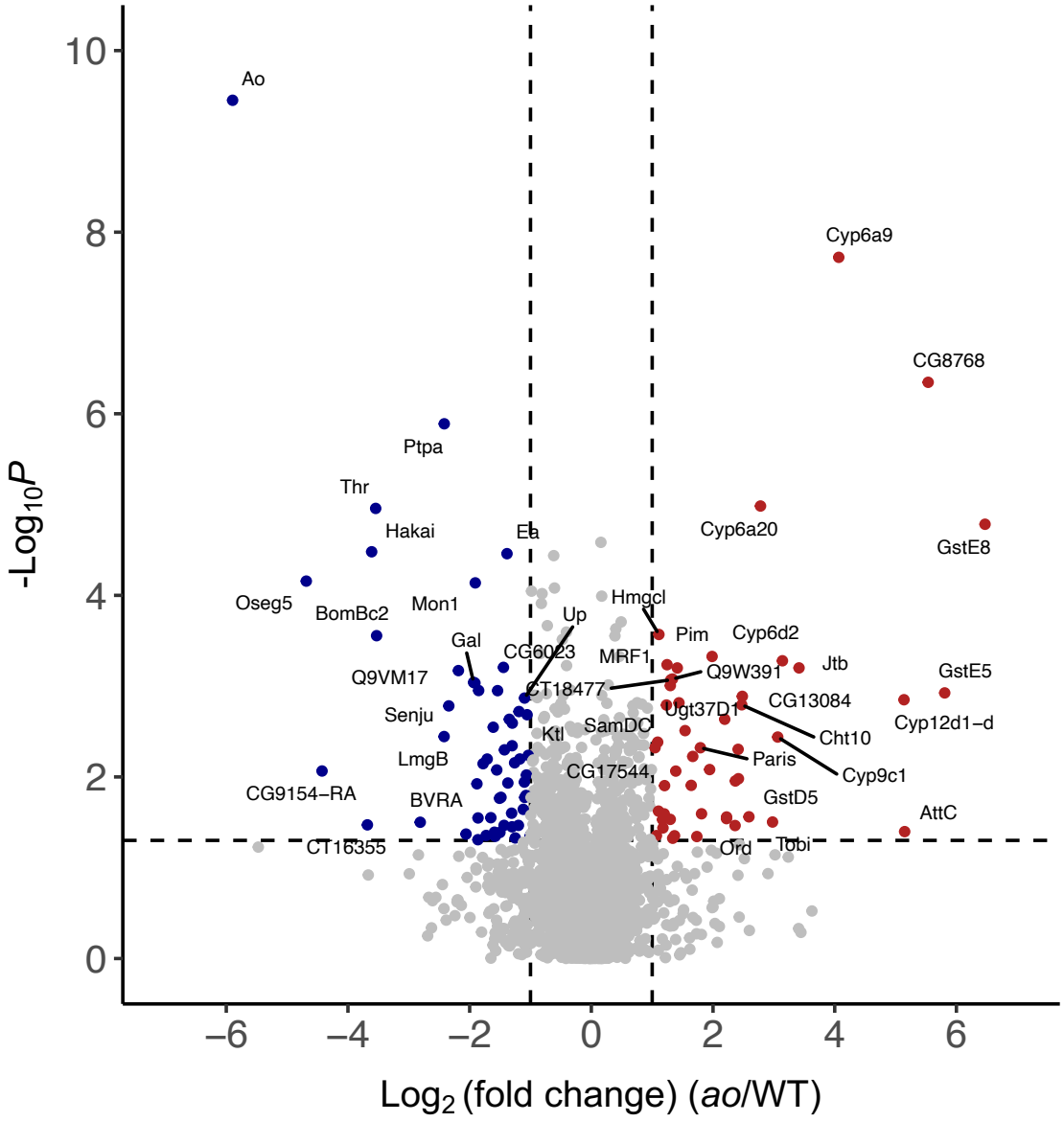

Figure 3.2: Proteins identified in tandem mass tag mass spectrometry with Δ*ao* ovaries. 6,691 total proteins were identified. Proteins in red have log_2(fold change) > 1.0 and *p*-value < 0.05; 17 of these have FDR < 0.10. Proteins in blue have log_2(fold change) < -1.0 and *p*-value < 0.05. WT is the isogenic *yw* flies.

Protein	Fold Change (*ao*/WT)	*p*-value	FDR
Cyp6a9	16.76	1.89E-08	6.33E-05
CG8768	46.40	4.51E-07	1.00E-03
Cyp6a20	6.87	1.04E-05	1.23E-02
GstE8	88.70	1.65E-05	1.58E-02

Table 3.3: Proteins identified in TMT MS with $\log_2$(fold change) > 1.0 and FDR < 0.05.

Protein	Fold Change (*ao*/WT)	*p*-value	FDR
Ao	0.02	3.53E-10	2.36E-06
Ptpa	0.19	1.29E-06	2.16E-03
Thr	0.09	1.10E-05	1.23E-02
Hakai	0.08	3.31E-05	2.22E-02
Ea	0.38	3.48E-05	2.22E-02
Mon1	0.27	7.29E-05	3.75E-02
Oseg5	0.04	6.97E-05	3.75E-02

Table 3.4: Proteins identified in TMT MS with $\log_2$(fold change) < -1.0 and FDR < 0.05.

For the initial analysis, we only focused on the proteins with FDR < 0.05 and $\log_2$ fold change > 1.0 (for more abundant proteins) or < -1.0 (for less abundant proteins). We looked for essential proteins whose mutant phenotypes mirrored Ao's. We prioritized genes whose mutations also caused maternal-effect lethality and defects at the embryonic stage, particularly at the midblastula transition when offspring from ao^1 mothers manifest defects (Chari et al. 2019), or in late embryogenesis after cuticle deposition and before hatching, when lethality in offspring from ao^1/ao^1 and ao^1/ao^2 mothers was observed (Sullivan 1985; Tomkiel et al. 1995). We identified three proteins that met these criteria. All three of these proteins – Three rows, Hakai, and Easter – are less abundant in the Δ*ao* ovaries and may represent indirect targets of Ao.

Three rows (fold change = 0.09, FDR = 1.23E-02) is a component of the *Drosophila* separase complex, which cleaves cohesin and thereby allows for the separation of sister chromatids during mitosis (Leismann et al. 2000, Jäger et al. 2001). *three rows* is zygotic lethal, with homozygous mutants exhibiting defects at nuclear cycle 15 (D'Andrea et al. 1993). It also has a maternal

effect, as the maternal protein is sufficient for viability until nuclear cycle 15 during embryogenesis (D'Andrea et al. 1993).

Hakai (fold change = 0.08, FDR = 2.22E-02) encodes a RING E3 ubiquitin ligase and was initially identified as an E-cadherin-binding protein in humans (Fujita et al. 2002). In *Drosophila*, the maternal Hakai protein is essential for epithelial integrity in the embryo; most offspring from *Hakai*-mutant mothers, regardless of paternal genotype, are embryonic lethal (Kaido et al. 2009). Offspring from *Hakai* homozygous-mutant mothers undergo oogenesis, but most die before hatching owing to epithelial defects ranging from unformed denticles to the near-absence of exoskeletons (Kaido et al. 2009).

Easter (fold change = 0.38, FDR = 2.22E-02) encodes a secreted serine protease implicated in the Toll pathway. It is required for the establishment of the dorsal-ventral axis in embryos (Chasan and Anderson 1989, Misra et al. 1998, Cho et al. 2010). *easter* is maternal-effect lethal, and *easter* homozygous-mutant mothers produce dorsalized embryos (Chasan and Anderson 1989).

Δ*ao* flies do not have increased histone protein levels

Given that Ao's *Arabidopsis* and human orthologs are involved in histone ubiquitination (Nassrallah et al. 2018, Wang et al. 2006), our finding no evidence of *ao* affecting histone transcripts, and *ao*'s genetic interaction with the histone gene array (Berloco et al. 2001, Chapter 2 of this dissertation), we wondered whether Ao might also regulate histones post-translationally.

In the TMT MS experiment, we found no difference in core (Table 3.5) or variant (Table 3.6) histone levels between Δ*ao* and wildtype ovaries. The pull-down MS did not identify core or variant histones that interacted significantly with Ao-HA (Table 3.7). To verify these results, we quantified the amounts of H2B and H3 protein in Δ*ao* and isogenic-wildtype ovaries with western blots. We found no significant difference in H2B protein levels between Δ*ao* and wildtype ovaries (Fig 3.3). Somewhat surprisingly, Δ*ao* ovaries had a two-fold decrease in H3 levels relative to wildtype ovaries (Fig 3.3). Upon scanning the H3 blots at higher intensity, we observed bands that correspond in molecular mass to ubiquitinated histones (~15kDa for H3 plus increments of 8.6kDa for ubiquitin). Further experiments are needed, however, to determine

whether these bands truly originate from the H3 antibody (both H3 and tubulin antibodies recognize the same secondary antibody, and both antibodies are polyclonal). If these bands indeed represent ubiquitinated H3, the decrease in unmodified H3 levels for Δ*ao* ovaries might indicate that the total amount of H3 proteins does not change in the absence of *ao*, but that the amount of ubiquitinated H3 increases. No such bands were observed for the H2B blot.

Histone	**Fold Change (*ao*/WT)**	***p*-value**	**FDR**
His2A	0.90	0.15	0.73
His2B	0.91	0.21	0.76
His3	0.97	0.54	0.82
His4 and His4r	0.91	0.81	0.94
His1	1.02	0.74	0.91

Table 3.5: Core histones identified in TMT MS.

Histone variant	**Fold Change (*ao*/WT)**	***p*-value**	**FDR**
His2Av	0.66	0.05	0.61
His3.3A	1.14	0.03	0.55
Cid	1.60	0.48	0.80
BigH1	1.08	0.68	0.89

Table 3.6: Variant histones identified in TMT MS.

Histone	***Fold change (ao-HA/nls-GFP)***	***p-value***	***FDR***
His1	1.64	8.12E-01	0.873
His2Av	0.70	3.95E-02	0.324
His2B	0.57	2.02E-01	0.439
His3.3A	0.38	2.32E-02	0.315
His4 and His4r	1.00	4.37E-01	0.604

Table 3.7: Core and variant histones identified in pull-down MS.

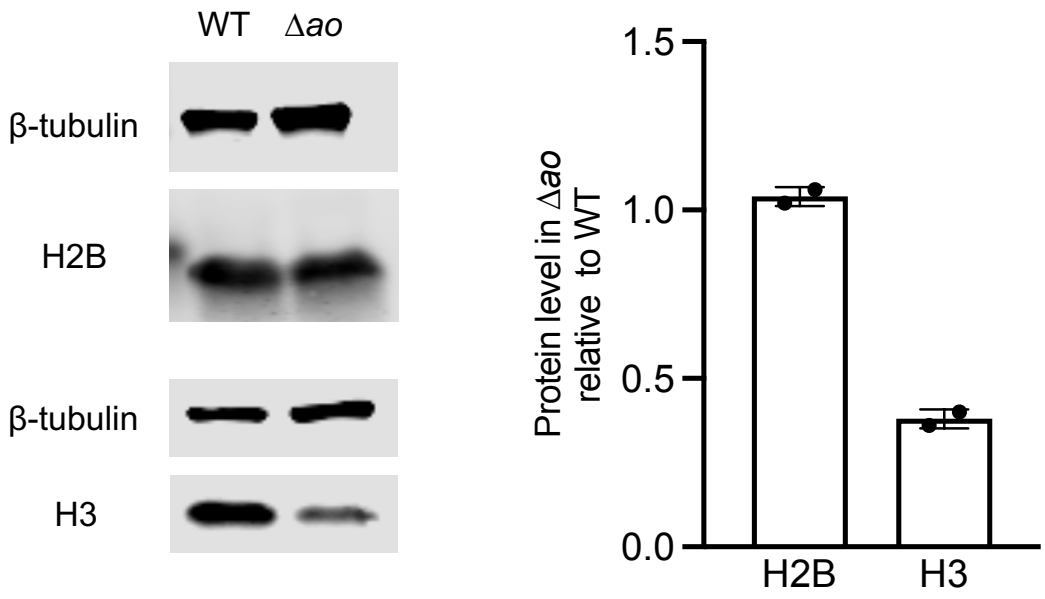

Figure 3.3: Western blots for H2B and H3 on Δ*ao* and wildtype ovaries. There is no difference in H2B levels between Δ*ao* and WT ovaries, whereas the amount of H3 is lower in Δ*ao* ovaries relative to WT. The values have been normalized to Beta-tubulin. WT is the isogenic *yw* flies.

3.4: Discussion

Orthologs of Ao include the *Arabidopsis* DET1, which functions as a negative regulator of light-mediated growth in seedlings (Chory et al. 1989, Chory and Peto 1990, Pepper et al. 1994) and human hDET1, which is a negative regulator of the proto-oncogene c-Jun (Wertz 2004, Pick et al. 2007). Both the plant and mammalian DET1 are components of the COP1-CUL4A-RING E3 ubiquitin ligase complex (Yanagawa et al 2004, Bernhardt et al. 2006, Wertz et al. 2004, Pick et al. 2007). Given the conserved mechanisms of the plant and mammalian DET1 proteins, we hypothesized that *Drosophila* Ao also functions as a post-translational, rather than transcriptional, regulator (although it may also indirectly affect translation by targeting the degradation of a transcriptional factor).

Even at the post-translational level, our findings reveal that Ao does not directly affect histone levels; histone protein levels are unaffected in Δ*ao* mutant ovaries based on our TMT MS experiment. Furthermore, none of the core histones were pulled down in the MS assay with *ao*-HA ovaries (although H1 was identified at lower statistical significance). The H4 variant His4r, which is identical in sequence to core histone H4, was identified as Ao's potential interactor in

the yeast two-hybrid assay (albeit with low confidence scores). We also considered the possibility that Ao is involved in histone ubiquitination, based on *Arabidopsis* DET1's role in H2B monoubiquitination and human hDET1's possible role in H3 and H4 polyubiquitination (Nassrallah et al. 2018, Wang et al. 2006). Indeed, increased exposure of western blots for H3 revealed bands that are consistent with polyubiquitinated H3 proteins. However, additional experiments are required to conclude that they indeed result from the H3 antibody, and that they are more abundant in Δ*ao* ovaries relative to wildtype ovaries. If true, the ubiquitination of histones could result in their more facile eviction from nucleosomes, potentially explaining why a decrease in histone copy number rescues the *ao* maternal-effect lethality.

Although the H3 ubiquitination hypothesis is tantalizing, we speculate that Ao may also target a different cellular protein(s), whose perdurance in ovaries leads to maternal-effect lethality. Cul4 E3 ligases often have multiple targets, including the human CUL4-DDB-ROC1 complex, which ubiquitinates both histones (Wang et al. 2006) and c-Jun (Wertz et al. 2004). Identification of this (still unknown) Ao target might also reveal why reduced histone copy number and excess AO heterochromatin rescue *ao*'s maternal-effect lethality.

Two tantalizing targets are revealed by the TMT MS experiment. The first of these is Hakai. In addition to its maternal-effect lethal phenotype, Hakai assembles in the same E3 complex with Mettl4, the protein that displayed the most significant affinity with Ao in the pull-down MS experiment. Hakai and Mettl14 belong to the "writer" complex of the N6-methyladenosine (m^6A) modification pathway, which adds a methyl group to the N6 position of adenosine residues in RNA molecules and is the most common mRNA-modification pathway in eukaryotes (Wang et al. 2001, Bawankar et al. 2021). Hakai and Mettl14 were shown to interact in a co-IP experiment in *Drosophila* S2 cells (Wang et al. 2001). However, knocking down *Hakai* in *Drosophila* S2 cells (Bawankar et al. 2021) or in the wing disc *in vivo* (Wang et al. 2001) did not affect Mettl14 protein levels. Furthermore, the absence of Hakai leads to the degradation of other proteins in the m^6A "writer" complex (Wang et al. 2021). We did not observe a significant change in the level of Fl(2), Vir, or Flacc proteins, which are known to decrease in the absence of Hakai (Wang et al. 2001, Bawankar et al. 2021). For these reasons, the identification of Hakai in the TMT MS and Mettl14 in the pull-down MS, though intriguing, might be a red herring in the dataset.

A more promising candidate of Ao's target is Three rows, which encodes a *Drosophila* separase. Unlike most eukaryotes, *Drosophila* has two separase proteins: Three rows (Thr) and Separase (Sse), which correspond to the N- and C-terminal regions, respectively, of a single-chain separase in other species (Jäger et al. 2001). Thr and Sse form a complex with Pimples (Pim), the *Drosophila* securin, that is essential for the separation of sister chromatids during mitosis (Leismann et al. 2000, Jäger et al. 2001). Successful separation of sister chromatids depends on the degradation of Pim, which accumulates during interphase and degrades after the mitotic metaphase/anaphase transition (Stratmann and Lehner 1996, Leismann et al. 2000). Both the overexpression of *pim* and high levels of nondegradable Pim inhibit sister chromatid separation and are lethal (Leismann et al. 2000). Although there are no data demonstrating the effects of *pim* overexpression on *thr*, the degradation of securin via ubiquitylation is required before the activation of separase in human cells and in yeast (Hornig et al. 2002, Waizenegger et al. 2002). In both systems, securin prevents substrates from binding to the active sites of separase (Hornig et al. 2002, Waizenegger et al. 2002). In our TMT MS experiment, we observed a 4-fold increase in Pim and 11-fold decrease in Thr in Δ*ao* ovaries relative to wildtype. Furthermore, *thr* is maternal-effect lethal; maternal Thr is sufficient for viability until nuclear cycle 14 during embryogenesis, coinciding with the onset of the midblastula transition at nuclear cycle 13-14, when zygotic-gene activation commences (D'Andrea et al. 1993, Philip et al. 1993, Yuan et al. 2016).

These data together suggest a hypothesis that Ao is involved in the regulation of Thr. One possible mechanism, based on the TMT MS data, is that Ao is the substrate-recognition subunit of an E3 ligase that targets Pim for degradation. In this framework, the absence of Ao results in an excess of Pim, which results in a decrease in Thr, ultimately leading to unsuccessful mitosis and embryonic death. Alternatively, Ao could be involved in the modification of a different protein that affects the expression of Thr. We plan to test this hypothesis, as well as the mechanisms underlying the hypothesis, via three approaches. First, we will validate the TMT MS results by running western blots on Δ*ao* ovaries with Thr and Pim antibodies. In tandem, we will test *in vivo* whether overexpressing *thr* can rescue the maternal-effect lethality of Δ*ao* flies. Finally, we performed an experimental evolution experiment with Δ*ao* flies to determine whether the naturally occurring suppressors of the *ao* phenotype (Krider and Levine 1975) have any connections to Thr or Pim. This last experiment is discussed in further detail in Chapter 4.

3.5: Materials and methods

Pull-down MS sample preparation

To obtain the *ao-HA* fly to use in the pull-down MS experiment, we crossed the UAS-*ao-HA* line (FlyORF F001850) to the maternal triple driver (MTD)-GAL4 line (BDSC 31777). To obtain the *GFP-nls* control flies, we crossed the MTD-GAL4 driver to a UAS-*GFP-nls* responder line (BDSC 4776). We dissected ovaries in Grace's insect media (Thermo) on ice. We prepared each genotype in biological triplicates, with n=85 to 100 pairs of ovaries per replicate sample. We ground the tissue with a pestle in lysis buffer (50 mM pH8.0 Tris, 137 mM NaCl, 1 mM EDTA, 1% Triton X-100, 10% glycerol, 10 mM NaF) with protease inhibitor (Roche). We centrifuged the samples at maximum speed for 15 minutes at 4°C, collected the lysate, and repeated this step until the lysate was clear. The samples were stored at 4°C for 2 weeks prior to immunoprecipitation (owing to failed quantification attempts). We performed the immunoprecipitation using the Pierce anti-HA agarose beads (Thermo). After three washes in lysis buffer to remove the storage, we added 80µL of bead slurry per 350µL of lysate, and incubated overnight on a nutator at 4°C. The samples were centrifuged at 2000g for 2 minutes at 4°C, then the beads were washed four times with lysis buffer on a nutator at 4°C (20 minutes per wash). We added 40µL of loading buffer to 40µL of beads, then eluted by boiling at 95°C for 10 minutes. We ran the samples on the Any kD Mini-PROTEAN TGX Precast Protein Gel (Bio-Rad Laboratories). After three 5-minute washes in water, the gel was stained with Coomassie blue (Bio-Rad Laboratories) overnight, then washed three times with water (1 hour per wash). We cut the 62kDa Ao protein from the gel for further extraction and preparation at the Fred Hutch Proteomics and Metabolomics Core.

TMT MS sample preparation

We dissected ovaries from 6-to-7-day-old virgin females in PBS on ice. We prepared each genotype in biological triplicates, with n=7 pairs of ovaries per replicate sample. We lysed the samples in 60µL of RIPA buffer (Thermo) with protease inhibitor (EDTA-free cOmplete ULTRA Tablets, Roche) using an electric homogenizer and disposable pestle. The samples were centrifuged at the maximum speed for 15 minutes at 4°C, then the collected lysate was treated with 20 units of Pierce Universal Nuclease (Thermo) for 30 minutes at 37°C. The samples were stored at -80°C prior to quantification and analysis at the Fred Hutch Proteomics and

Metabolomics Core. The samples were quantified using the bicinchoninic acid (BCA) assay and extracted via methanol-chloroform precipitation.

Yeast 2-hybrid assay

The yeast two-hybrid assay was performed by Hybrigenic Services (Évry-Courcouronnes, France). The *ao* coding sequence tagged with GAL4 or LexA was screened against a cDNA library constructed from *D. melanogaster* ovaries. The LexA and Gal4 sequences were fused to the C- and N-terminal ends of *ao,* respectively, since LexA is known to work better on the C terminus and Gal4 o the N terminus (Petra Tafelmeyer, Hybrigenics, personal communication). After positive clones were sequenced, each interaction was assigned a confidence score between A and F, with A representing very high confidence in the interaction, and F representing experimentally proven technical artifacts.

Western blotting

We dissected ovaries from 4-day-old virgin females in PBS on ice. We transferred 5 pairs of ovaries to an Eppendorf tube, added 20µL of 2x Laemmli Buffer (Bio-Rad Laboratories) with 200 mM DTT and 300 mM NaCl, and flash froze the samples in liquid nitrogen. The samples were stored at -80°C until ready to be processed. To extract protein, we thawed the samples on ice and added protease inhibitor (EDTA-free cOmplete ULTRA Tablets, Roche), then hand-pestled the samples on ice using disposable pestles. After a brief spin at 4°C to collect the samples, we boiled the samples at 100°C for 10 minutes, then centrifuged the samples at maximum speed for 2 minutes to obtain clean lysate.

We loaded 10µL of protein sample per well on the Any kD Mini-PROTEAN TGX Precast Protein Gel (Bio-Rad Laboratories). We ran the gel for 90 minutes at 100V in Tris/Glycine/SDS buffer, then transferred the gel to a Trans-Blot Turbo Mini 0.2µm Nitrocellulose membrane (Bio-Rad Laboratories) using the Trans-Blot Turbo Transfer System (Bio-Rad Laboratories). The membrane was washed three times with PBS, blocked in Intercept (PBS) Blocking Buffer (LI-COR) for 1 hour at room temperature, then probed with primary antibodies in phosphate-buffered saline with 0.1% Tween-20 (PBST) at 4°C overnight. We used the following primary antibodies: rabbit anti-beta tubulin (abcam 6046) at [1:1000], mouse anti-H2B (abcam 52484) at [1:3000], and rabbit anti-H3 (abcam 1971) at [1:4000]. Following three 10-minute washes in

PBST, the membrane was incubated for 1 hour at room temperature with IRDye 680RD Donkey anti-Mouse IgG (LI-COR) and/or IRDye 800CW Donkey anti-Rabbit IgG 800 (LI-COR) secondary antibodies in PBST at [1:20,000]. After three washes with PBST and a final wash in PBS, we scanned the membrane at 700nm and 800nm on the Odyssey CLx Imager (LI-COR).

3.6: Acknowledgements

I thank Phil Gafken, Brian Milless, and Chenwei Lin at the Fred Hutch Proteomics and Metabolics Core for their assistance with the TMT MS and pull-down MS experiments; Hybrigenics Services (Évry-Courcouronnes, France) for performing the yeast two-hybrid assays; Marianne Mercer (Buszczak lab, UT Southwestern) for sharing her protocol for pull-down MS sample preparation; Aida de la Cruz and Sierra Simmerman (Malik lab, Fred Hutch) for helping dissect the *Drosophila* ovaries for the pull-down MS experiment; and Janet Young (Malik lab, Fred Hutch) for help with visualization of the MS dataset.

Chapter 4: Suppressors of *ao*

4.1: Abstract

ao-mutant flies suffer maternal-effect lethality. Yet, when kept as homozygous stocks, some *ao*-mutant fly strains spontaneously acquire a suppressor that restores fitness by significantly ameliorating *ao*'s maternal-lethal phenotype. This 'suppressor' phenotype has been replicated in multiple studies since its discovery in 1975. However, the genomic change(s) underlying this phenotype remained understudied. We conducted an experimental evolution experiment to identify novel loci that could act as *ao*'s suppressors using the protocols previously established for Δ*ao* flies. We propagated nine independent Δ*ao* stocks for 30 generations, then conducted fertility assays to determine the degree of maternal-effect lethality in each line. Some lines had acquired a robust suppression of the maternal-effect phenotype, whereas others remained just as unfit as the parental strain. We then investigated genomic differences between 'suppressor' and 'non-suppressor' lines using whole-genome sequencing. We discuss preliminary results from these ongoing analyses, which promise to reveal insights into mechanisms of suppression of Δ*ao*-associated maternal-effect lethality and, ultimately, the mechanisms by which Δ*ao* manifests maternal-effect lethality.

4.2: Introduction

In 1975, a study by Hallie Krider and Bryan Levine revealed a novel, perplexing phenotype of *ao*: ao^1 flies kept in homozygous stocks spontaneously acquired genetic suppressors, such that between the 5th and 12th generations, ao^1 mutant mothers produced an equal amount of male and female offspring when mated to attached X^Y males (Krider and Levine 1975). When these suppressor-bearing flies were crossed to flies with a 2nd chromosome balancer (*CyO*) and maintained as heterozygotes, the number of flies bearing the suppressor phenotype steadily decreased; by the 6th generation, 60% of the ao^1-homozygous mothers had reverted to producing an excess of female offspring when mated to attached X^Y males (Krider and Levine 1975). Given the plasticity (both directional and temporal) of the suppressor phenotype, as well as prior reports about excess X-chromosome heterochromatin rescuing *ao*'s maternal-effect lethality

(Sandler 1970, Parry and Sandler 1974, Sandler 1977), Krider and Levine suspected that the expansion of the genomic rDNA array, which codes for 18S, 28S, and 5.8S ribosomal RNAs (Ritossa et al. 1965, Tautz et al. 1988), might underlie the suppression phenotype. They compared the rDNA copy number between the *ao* flies with the suppressor and *ao* flies kept in the heterozygous stock. They found that the *ao* flies with the suppressor phenotype indeed had an expansion of the rDNA array (nearly a seven-fold increase in suppressor-bearing females kept as homozygotes for 12-15 generations), suggesting that an increase in rDNA copy number might have been responsible for the suppressor phenotype (Krider and Levine 1975).

Subsequent studies observed a similar phenomenon of *ao* mutants developing suppressors when maintained as homozygous stocks. Some of these studies found additional evidence supporting the finding that rDNA expansions occurred in 'suppressor' stocks (Krider et al. 1979; Graziani et al. 1981). However, others challenged the view that the expansion of the rDNA locus caused the suppressor phenotype, suggesting that changes in heterochromatic regions other than the rDNA could be responsible for the suppressor effect (Yedvobnick et al. 1980, Manzi et al. 1986, Sullivan and Pimpinelli 1986). Because the rescue factors that arise in *ao* homozygous stocks act additively (Sullivan and Pimpinelli 1986), copy number changes in (unknown) rescue genes located in the heterochromatin were proposed to underlie the suppressor phenotype (Sullivan and Pimpinelli 1986). Furthermore, the observations that the suppressor phenotype fixes quickly within the population – within 5 to 12 generations (Krider and Levine 1975) – bolstered the hypothesis that copy number changes, whether in rDNA, satellite DNA, histones, or some other repetitive array, might underlie the suppressor.

Given that deficiency in histone genes rescues maternal-effect lethality in ao^1 and Δ*ao* flies (Berloco et al. 2001; Chapter 2 of this dissertation), we hypothesized that a reduction in histone gene copy numbers could consistently underlie the *ao* suppressor phenotype. However, we entertained the possibility that multiple, different changes in the genome – including the expansion of the rDNA locus, reduction of histone gene copy number, changes in satellite DNA, or even point mutations in heterochromatin-interacting genes – could contribute to the *ao* suppressor phenotype. To explore these possibilities, we replicated the historical experimental-evolution experiment with our Δ*ao* flies and used whole-genome sequencing to interrogate changes in the genome of the suppressed *ao* flies.

4.3: Results

A fraction of Δ*ao* homozygous stocks develop the suppressor phenotype

We set up 10 replicate vials of Δ*ao*-homozygous stocks. We maintained the homozygous stocks for around 30 generations, following the methods from a previous study on ao^1 flies (Sullivan and Pimpinelli 1986). One of the vials had no remaining offspring after the fourth generation. This occurrence is not unexpected given the Δ*ao*-associated maternal-effect lethal phenotype. After ~30 generations, we conducted fertility assays on the remaining nine vials to test for the presence of a suppressor. A previous study had reported no suppressors on the Y chromosome (Sullivan and Pimpinelli 1986); however, we wished to maintain an agnostic approach. Therefore, we first tested the fertility of Δ*ao* females crossed to Δ*ao* males of the same stock. We found that three of the nine homozygous stocks had a robust increase in fertility relative to Δ*ao* flies maintained as heterozygotes (Mann-Whitney U test, $p < 0.05$), indicating the potential acquisition of a suppressor mutation in at least three strains (Fig 4.1).

We next crossed the Δ*ao* females from the homozygous stocks to males with an attached X^Y chromosome (BDSC 9460) to assay the offspring sex ratio. We found that females from two homozygous stocks produced an offspring sex ratio that deviated from the ratio of Δ*ao* females from the heterozygous stock (2x2 contingency table with Fisher's exact test, p-value < 0.10), indicative of a potential suppressor (Fig 4.2). Only line 9 was significant in both fertility assays. However, given the high variance and low replicate numbers in the dataset, the statistical power of the dataset is likely low. Moreover, the attached X^Y cross cannot evaluate any potential suppressors that might have arisen on the original X, and especially, Y chromosomes in the Δ*ao* stock.

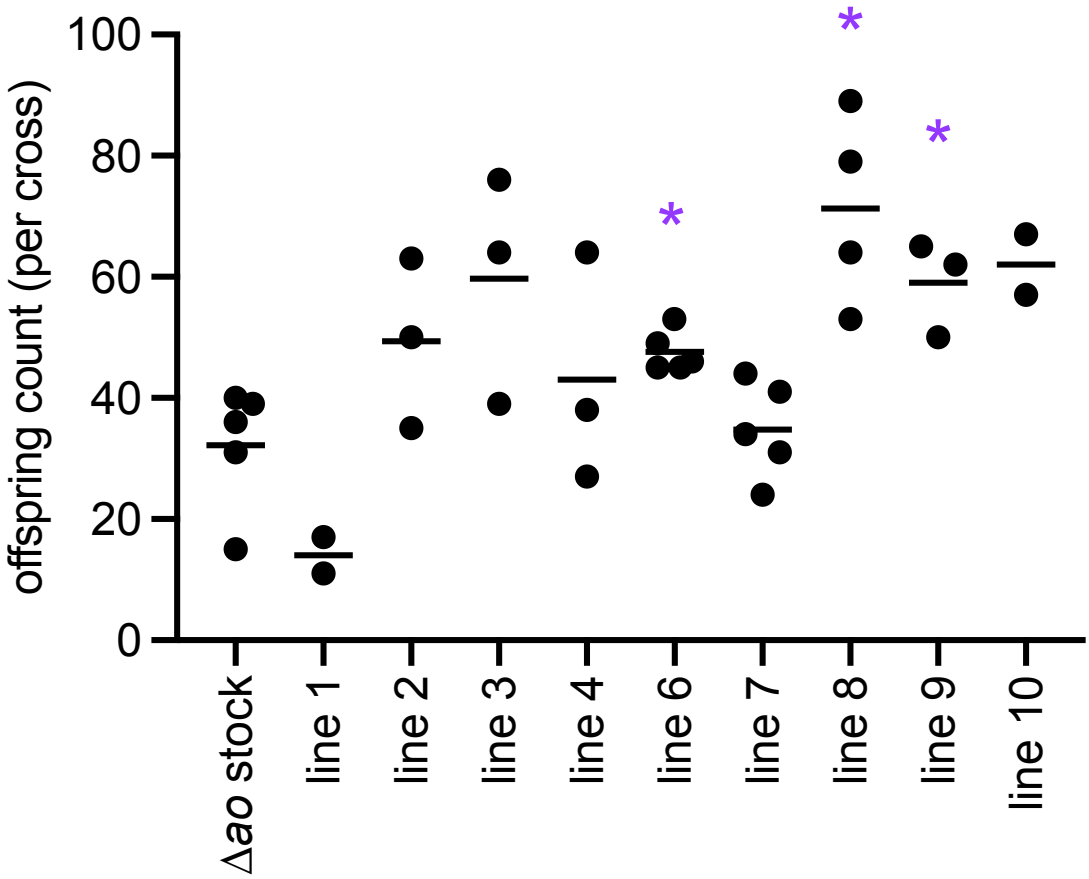

Figure 4.1: Fertility assay on Δ*ao* lines kept in homozygous stocks for ~30 generations. Δ*ao* stock refers to Δ*ao*/Δ*ao* flies that have been maintained in the heterozygous stock with the *CyO-GFP* balancer on the 2nd chromosome. Flies from lines 1 and 2 were at the 31st generation of the homozygous stock, flies from lines 3-10 were at the 29th generation, and flies from line 5 perished by the 5th generation and were therefore not assayed. All fertility crosses were conducted on the same day. Offspring counts of lines 6, 8, and 9 (purple asterisks) were statistically significant compared to Δ*ao* stock (Mann-Whitney U test, $p < 0.05$). The line represents the mean.

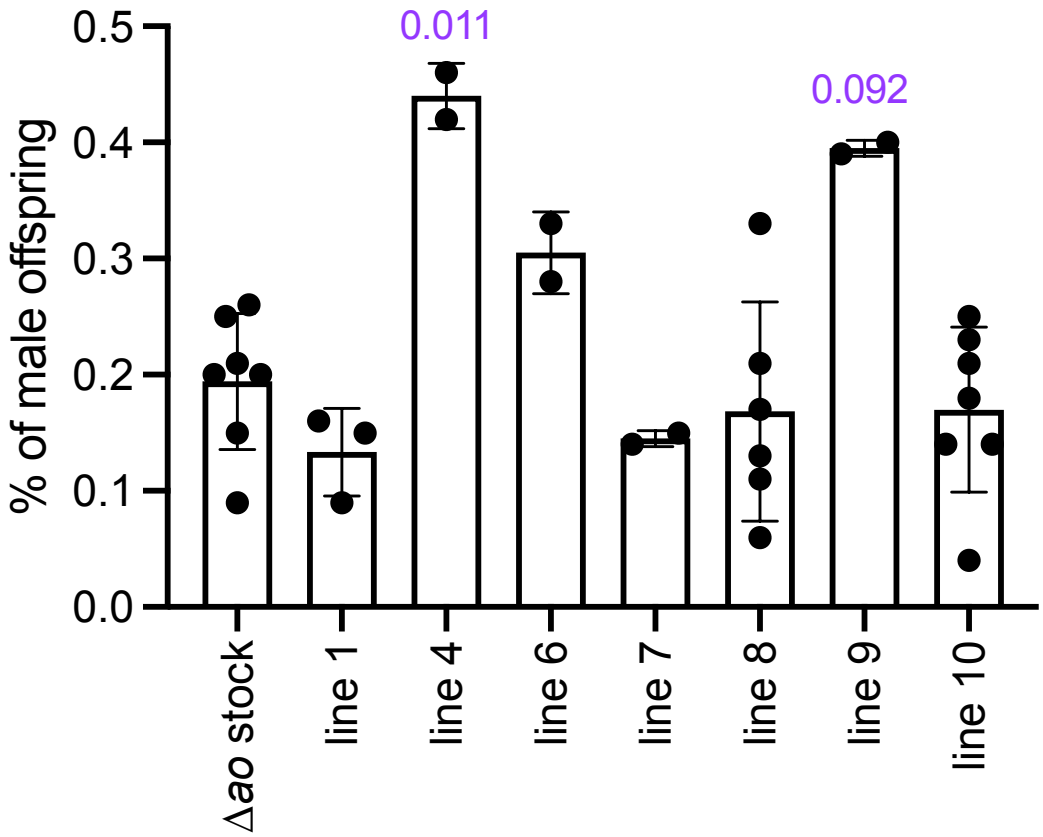

Figure 4.2: X^Y cross on Δ*ao* lines kept in homozygous stocks for ~30 generations. Δ*ao* stock refers to Δ*ao*/Δ*ao* flies that have been maintained in the heterozygous stock with the *CyO-GFP* balancer on the 2nd chromosome. Females from lines 1 were at the 35th generation of the homozygous stock, and from lines 3-10 were at the 33rd generation. Attached X^Y males are BDSC 9460. All fertility crosses were conducted on the same day. *p*-values are from the 2x2 contingency table with two-tailed Fisher's exact test. The line represents the mean with the standard deviation.

Genomic analysis of Δ*ao* suppressor lines

We collected genomic DNA from whole males in each of the (suppressor and non-suppressor) Δ*ao* lines for whole-genome sequencing analysis. (We used males to allow for the identification of suppressors on the Y chromosome.) Because lines 1 and 2 were established earlier than lines 3 to 10, flies from lines 1 and 2 were in the 32nd generation, whereas those from lines 3 to 10 were in the 30th generation. PCR-free library preparation and Illumina sequencing were conducted by Novogene Corporation Inc. (Sacramento, CA). Preliminary analysis of the data indicates that neither histone copy number (Fig 4.3) nor rDNA copy number (either 35S on the X chromosome or 5S on the 2nd chromosome, Fig 4.4) differs between Δ*ao* flies with the suppressor phenotype and Δ*ao* flies kept in the heterozygous stock. Analysis of the rest of the genome, including SNPs in potential protein-coding genes, is underway.

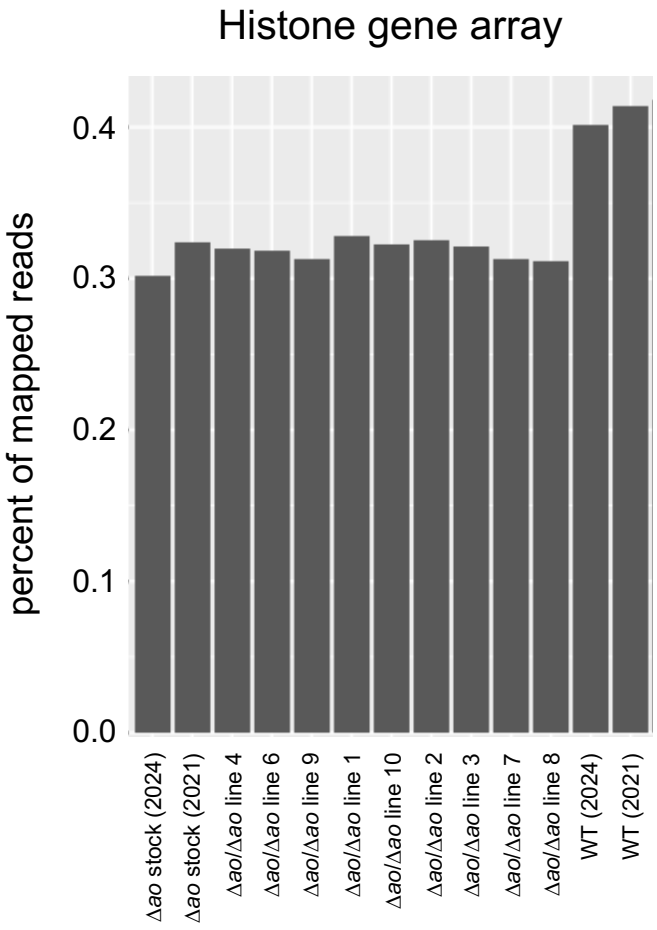

Figure 4.3: No change in histone copy number between Δ*ao* flies maintained in homozygous and heterozygous stocks. Δ*ao* stock refers to Δ*ao*/Δ*ao* flies that have been maintained in the heterozygous stock with the *CyO-GFP* balancer on the 2nd chromosome. WT refers to the isogenic *yw* flies with wildtype *ao*. Δ*ao* stock and WT flies collected and sequenced separately in 2021 were included in the analysis for comparison.

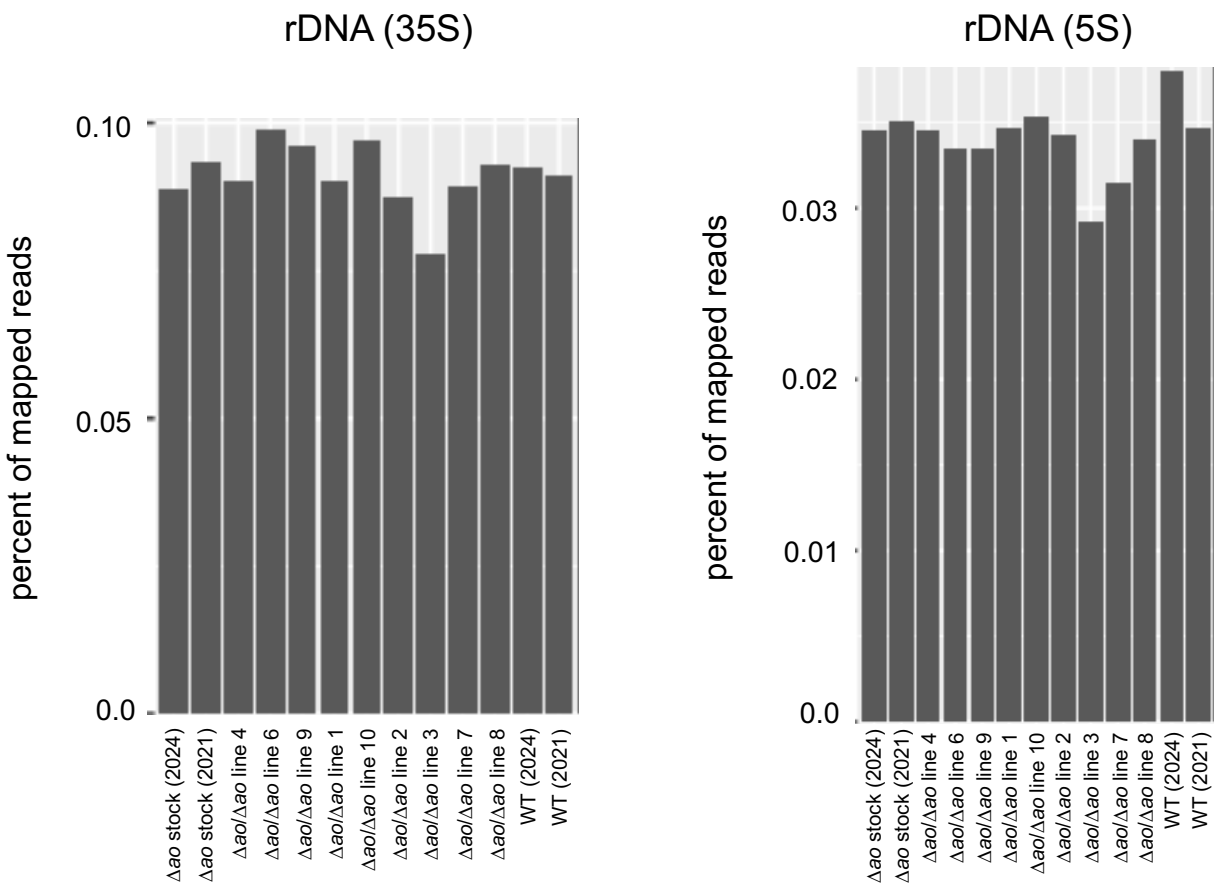

Figure 4.4: No change in rDNA copy number between Δ*ao* flies maintained in homozygous and heterozygous stocks. 35S is located on the X chromosome, and 5S is on the 2nd chromosome. Δ*ao* stock refers to Δ*ao*/Δ*ao* flies that have been maintained in the heterozygous stock with the *CyO-GFP* balancer on the 2nd chromosome. WT refers to the isogenic *yw* flies with wildtype *ao.* Δ*ao* stock and WT flies collected and sequenced separately in 2021 were included in the analysis for comparison.

4.4: Discussion

We experimentally evolved Δ*ao* flies in homozygous stocks for over 30 generations and found that some, but not all, homozygous stocks acquired a suppressor(s), which rescued *ao*'s maternal-effect phenotype. Contrary to previous studies (Yedvobnick et al. 1980, Manzi et al. 1986, Sullivan and Pimpinelli 1986), whole-genome sequencing of our experimentally evolved Δ*ao* lines revealed no changes in either histone copy number or rDNA copy number (at either 35S or 5S rDNA loci) in 'suppressor' Δ*ao* stocks.

We anticipated that the suppression phenotype might be associated with *de novo* variation that arose during the experimental evolution passaging. However, whole-genome sequencing of each surviving replicate line also revealed considerable standing variation still present on the 3rd and segments of the X chromosome. This variation is likely a result of the original variants present in the *yw* stock used to generate the Δ*ao* knockout on the 2nd chromosome, following which all variation on the 2nd chromosome was eliminated by homozygosity of this chromosome. Since considerable heterozygosity survived on the 3rd and X chromosomes, it is also possible that instead of *de novo* variation, selection to suppress the Δ*ao*-associated lethality may have acted on standing variation already present within the line, increasing the frequency of alleles associated with suppression. This might also provide an alternate explanation for why the suppressor phenotype fixes relatively quickly within the population(s).

Given the frequency of the suppressor phenotype and that the suppressor phenotype fixes relatively quickly within the population(s), we anticipate that a change in gene or satellite DNA array copy number is still the most likely candidate underlying the phenotype. The change(s) likely lies within the heterochromatic regions; for example, increasing the AO heterochromatic elements on the X, Y, and 2nd chromosomes has been demonstrated to rescue the *ao* maternal-effect lethality (Parry and Sandler 1974, Sandler 1977, Haemer 1978, Yedvobnick et al. 1980, Pimpinelli et al. 1985, Tomkiel et al. 1991). Thus, a duplication or copy-number expansion of the satellite DNA associated with the AO heterochromatin would parsimoniously explain the rise of the suppressor phenotype in the suppressed lines. Alternatively, missense or nonsense mutations in protein-coding genes identified in the RNA-seq analyses (Appendix A), pull-down and mass-spectrometry proteomics experiments (Chapter 3), or heterochromatin-interacting proteins could explain the suppressor phenotype. Finally, it is possible that the suppressor phenotype arises

from the interaction of multiple changes, including both standing variation and *de novo* mutations – either changes in copy number or point mutations – in the genome of the suppressed stocks. Furthermore, these changes might not be convergent, *i.e.,* different genomic changes lead to the same suppressed phenotype in different replicate populations. Although this is a less parsimonious explanation, lack of convergence might make it difficult to identify putative suppressor mutations and re-engineer them into Δ*ao* strain to causally demonstrate suppression of maternal-effect lethality.

4.5: Materials and methods

Experimental evolution and fertility assays

We set up 10 replicates of Δ*ao*-homozygous stocks in January 2023. We maintained the vials on the benchtop at room temperature and flipped them every 2 weeks into new vials with corn syrup/soy media.

We used 1-to-5-day-old males and virgin females for all fertility assays. To determine the offspring count of Δ*ao* flies kept in homozygous stocks, we paired 4 virgin females with 2 males in a vial with corn syrup/soy media and allowed them to mate for 1 week at 29°C. To prevent larval overcrowding in the vials, we flipped the parents to new vials after 3 days and discarded the parents from the new vials 4 days later. We counted the adult offspring (F1) to exhaustion. The following crosses were excluded from statistical analyses: 1) those with no larvae in one or both vials, and 2) those where 2 or more of the mothers, or 2 fathers, died during the 1-week mating period.

To determine the offspring sex ratio of Δ*ao* females kept in homozygous stocks, we set up a 1:1 mating of a Δ*ao* female with a X^Y male (BDSC 9460) in a vial with corn syrup/soy media and allowed them to mate for 1 week at 25°C. We scored the adult offspring (F1) to exhaustion. The following crosses were excluded from statistical analyses: 1) those with no larvae in one or both vials, and 2) those where either parent died during the 1-week mating period, and 3) those with F2, indicating that the parent male was not a true X^Y.

Because non-genetic factors, including variation in food and ambient humidity, influence fly fertility, we only compared data among the crosses set up on the same day. We used GraphPad Prism version 10.1.1 for macOS (GraphPad Software) to plot the data and conduct statistical analyses. To compare the total offspring count between the control (Δ*ao* flies maintained as a heterozygous stock) and an experimental line (Δ*ao* flies maintained as a homozygous stock), we performed two-tailed Mann-Whitney U tests and reported exact *p*-values. To compare the results of X^Y crosses, we analyzed a 2x2 contingency table using a two-tailed Fisher's exact test on the GraphPad website (https://www.graphpad.com/quickcalcs/contingency1/).

Whole-genome sequencing

We extracted genomic DNA from n=20 male carcasses in each of the suppressed lines using the DNeasy Blood & Tissue Kit (Qiagen) according to manufacturer for insect tissue using an electric motor and pestle. We treated the samples with RNAse A (Qiagen) for 1 hour at 37°C (1µL of 10mg/mL RNAseA per 100µL of DNA), then cleaned the samples with the Genomic DNA Clean & Concentrator-25 Kit (Zymo Research). We sent the DNA to Novogene Corporation Inc. (Sacramento, CA) for PCR-free library preparation and sequencing on the Illumina NovaSeq X Plus platform.

We used the BWA-MEM algorithm to map reads to the dm6 reference genome assembly (Li and Durbin 2010). For reads that mapped to multiple genomic locations, BWA will report one map location, choosing at random among equally well matching positions. We identified the coordinates of interest and created a bedfile and used bedtools multicov to count reads mapping to those regions. We divided the counts for each sample by the corresponding total number of mapped reads to obtain the proportion of reads deriving from the loci of interest.

4.6: Acknowledgements

I thank and Janet Young (Malik lab, Fred Hutch) for conducting the genomic analyses of Δ*ao* suppressor lines, and Sierra Simmerman (Malik lab, Fred Hutch) for conducting the fertility assays and assisting with maintenance of the homozygous-*ao* stocks.

Chapter 5: Perspectives and Prospectives

5.1: Dissertation summary

ao was recovered as a meiotic mutant from a natural *D. melanogaster* population and was initially described by Larry Sandler and colleagues in 1968 (Sandler et al. 1968). Sandler named the gene *abnormal oocyte* for the abnormal sex ratio mutant females produced when mated to males with an attached X^Y chromosome (Sandler 1970). Subsequent studies, including many by Sandler himself, demonstrated that increasing the dosage of specific regions of heterochromatin on the X, Y, and 2nd chromosomes, called AO heterochromatin, could ameliorate *ao'*s maternal-effect lethality (Parry and Sandler 1974, Sandler 1977, Haemer 1978, Yedvobnick et al. 1980, Pimpinelli et al. 1985, Tomkiel et al. 1991). The molecular mechanism behind *ao*'s maternal-effect lethality, as well as the relationship between the *ao* mutation and its rescue by AO heterochromatin, remained a mystery for over three decades after *ao'*s initial description. In 2001, a landmark study by Maria Berloco and colleagues concluded that *ao'*s maternal-effect lethality was caused by the overexpression of core histone transcripts (Berloco et al. 2001). This study reported that the Ao protein binds to the promoters of core histones to act as a transcriptional repressor and that decreasing histone copy number could partially rescue the maternal-effect lethality of *ao*-mutant mothers (Berloco et al. 2001). With this discovery, *ao* became a promising reagent to interrogate the effects of histone overexpression in a multicellular organism.

Existing *ao* reagents, however, had several associated caveats. Of the two *ao* strains characterized historically, only ao^1, the mutant recovered from the natural population, remains, whereas the lab-engineered ao^2 stock has been lost. ao^1 and ao^2, which differed in the position of the transposable-element insertion into the *ao* gene (insertion into the first exon and the promoter region, respectively), also differed in two key phenotypes: 1) ao^1 is viable as a homozygous mutant, whereas ao^2 was lethal as a homozygote (Tomkiel et al. 1995), and 2) a greater percentage of embryos from ao^1/ao^1 mothers died at earlier stages compared to those from ao^1/ao^2 mothers (Tomkiel et al. 1995). These differences in phenotype implied that one or both *ao* stocks had other lesions in their respective genetic backgrounds that confounded *ao*'s true phenotype.

To distinguish the *ao* phenotype from the background effects, I created a clean *ao* knockout using CRISPR/Cas9. Using the Δ*ao* flies, I found that contrary to prior evidence, *ao* is not a transcriptional repressor of core histones (Chapter 2). RT-qPCR experiments with both Δ*ao* and ao^1 ovaries showed that neither exhibited differences in histone expression relative to wildtype ovaries. Therefore, I speculate that ao^2, which was generated via *P*-element mutagenesis (Tomkiel et al. 1995), likely also acquired other mutations that led to the histone-transcript overexpression phenotype in the ao^1/ao^2 flies, whether independently or through its interaction with *ao.*

Given that Ao's plant and mammalian orthologs are E3 ligases, I hypothesized that Ao could also function as an E3 ligase instead of as a transcriptional repressor. I looked for putative targets of Ao using genetics and proteomics approaches (Chapter 3). I used pull-down mass spectrometry on tagged *ao* ovaries and the yeast two-hybrid assay to look for Ao's direct binding partners. I complemented these experiments by performing a tandem mass tag mass spectrometry experiment to look for Ao's degradation target. I developed several hypotheses, which are not necessarily mutually exclusive, based on these experiments. The most exciting of these hypotheses is that Ao regulates Three rows, one of the two *Drosophila* separase proteins, by targeting Pim, the *Drosophila* securin, for degradation. This model would explain the timing and phenotype of embryonic lethality of offspring from *ao*-mutant mothers, as well as the maternal-effect nature of the *ao* gene. Additional experiments will be required to confirm either this or other putative targets.

As an orthogonal approach to determine the target(s) of the *ao* product, as well as to elucidate the relationship between the *ao* mutation and the AO heterochromatin, I conducted an experimental-evolution assay to identify suppressors of *ao*'s maternal-effect phenotype (Chapter 4). I maintained Δ*ao* flies as homozygous stocks for 30 generations to allow the strains to evolve *de novo* suppressors of the maternal-effect phenotype. We conducted fertility assays and identified four independent lines where a suppressor might have evolved. We used whole-genome sequencing to look for genomic changes associated with losing *ao* maternal-effect lethality phenotype. Based on initial analyses, we found that neither histone nor rDNA copy-number change was associated with the *ao* suppressor phenotype. This raises the possibility that

additional loci, including potential changes in interacting protein-coding genes, may reveal a suppressor phenotype and shed further insight into *ao*-associated maternal-effect lethality.

5.2: Future directions

Although our findings challenge the molecular model of *ao* as a histone-transcript suppressor, we have reconfirmed its connection to histone copy number and heterochromatin. However, the basis of *ao*-associated maternal-effect lethality remains an open and exciting question.

A hypothesis derived from the proteomics experiments (Chapter 3) is that Ao targets Pim, the *Drosophila* securin, for degradation, leading to the loss of Three rows, the *Drosophila* separase. Although the effects of *pim* overexpression on the level of *thr* have not been tested, the degradation of securin is required to activate separase in humans and yeast (Hornig et al. 2002, Waizenegger et al. 2002). If this mechanism is also conserved in *Drosophila*, the absence of Ao could result in excess undegraded Pim, leading to the inactivation of Thr. To test this hypothesis, we plan to validate the proteomics results by running western blots on Δ*ao* ovaries for the Thr and Pim antibodies. We will also conduct a fertility assay with *thr*-overexpression flies to determine whether *thr* can rescue the *ao* maternal-effect lethality *in vivo.*

Furthermore, given that Ao's *Arabidopsis* and human orthologs are involved in histone ubiquitination (Nassrallah et al. 2018, Wang et al. 2006), and reduction in histone copy number ameliorates *ao*'s maternal-effect lethality (Berloco et al. 2001, Chapter 2), we plan to explore the possibility that Ao also ubiquitinates histones. Overexposure of western blots for the H3 antibody revealed bands that correspond in molecular mass to ubiquitinated histones (~15kDa for H3 plus increments of 8.6kDa for each ubiquitin moiety). In addition to follow-up Western blotting experiments, we plan to take a mass spectrometry approach to identify histone ubiquitination by isolating bulk histones from Δ*ao* ovaries and looking for known ubiquitinated sites on histones. If Ao does indeed ubiquitinate histones, either to target them for degradation or to modify their function, then a decrease in the ratio of ubiquitinated to unmodified histones might not only explain *ao*'s maternal-effect lethal phenotype but also explain why reducing histone copy number partially rescues the maternal-effect lethality. Additionally, if this model is true, then AO heterochromatic elements could rescue the *ao* maternal-effect lethality by acting as a sink for the unmodified histones.

Finally, the whole-genome sequencing dataset on the Δ*ao* flies with and without the suppressor phenotype (Chapter 4) requires further analyses. Although heterochromatic and repetitive regions pose bioinformatic challenges compared to mapping reads to euchromatic regions, recent assemblies and analyses have begun to elucidate the organization and structure of *Drosophila* heterochromatin (e.g., Shukla et al. 2024, Chang and Larracuente 2019). It is likely, given multiple independent data from genetic crosses (Krider and Levine 1975, Krider et al. 1979, Yedvobnick et al. 1980, Graziani et al. 1981, Manzi et al. 1986, Sullivan and Pimpinelli 1986) and the observations that the suppressor phenotype fixes quickly within the population, that changes in copy number of heterochromatic genes underlie the *ao* suppressor phenotype. Improved genomic assemblies of the *Drosophila* heterochromatin could help us identify the genetic cause of the *ao* suppressor phenotype.

When Larry Sandler characterized *ao* over five decades ago, it promised to reveal the mechanistic basis of genetic interactions between euchromatin, heterochromatin, and embryonic viability. Sandler held the view, inherited from his postdoctoral advisor Edward Novitski, that "nothing could be learned from cytology that could not be inferred from breeding experiments" (Lindsley 1999). Remarkably, the data from Sandler's carefully orchestrated genetic experiments on *ao* mutants (e.g., Sandler et al. 1968, Sandler 1970, Parry and Sandler 1974, Sandler 1977) remain the guiding posts in generating new hypotheses about its molecular mechanisms. In his recollection of Sandler, Dan Lindsley remarked that "Larry was unconcerned with the need to tackle popular topics; if the data posed an interesting question, that was incentive enough for him to accept the challenge" (Lindsley 1999). Although the data in this dissertation have provided some answers to the nature of the *ao* mutation, they pose even more questions. The new *ao* reagents we have created, as well as the dataset we have generated, will provide a new starting point for the next generation of curious researchers.

Appendix 1: RNA-sequencing of Δ*ao* flies

A1.1: Summary and results

We conducted RNA-sequencing experiments to detect genes expressed differentially between Δ*ao* and wildtype ovaries. We performed two RNA-seq experiments: one with a poly(A) library selection, which provides superior exonic coverage (Zhao et al. 2018), and another with ribosomal-depletion library preparation to capture core histones, which lack poly(A) tails (Marzluff et al. 2008).

The most differentially upregulated gene in Δ*ao* ovaries relative to wildtype in the poly(A) RNA-seq is *Drep1* (*DNA fragmentation factor-related protein 1*, Fig A1.1). *Drep1* is the *Drosophila* homolog of the human ICAD (also known as DFF-45), which is a substrate for caspase-3 and triggers DNA fragmentation during apoptosis (Inohara and Nunez 1999, Mukae et al. 2000). In *Drosophila, Drep1* is regulated maternally during embryogenesis, and acts as a negative regulator of apoptosis (Mukae et al. 2000, Yokohama et al. 2000, Park and Park 2013).

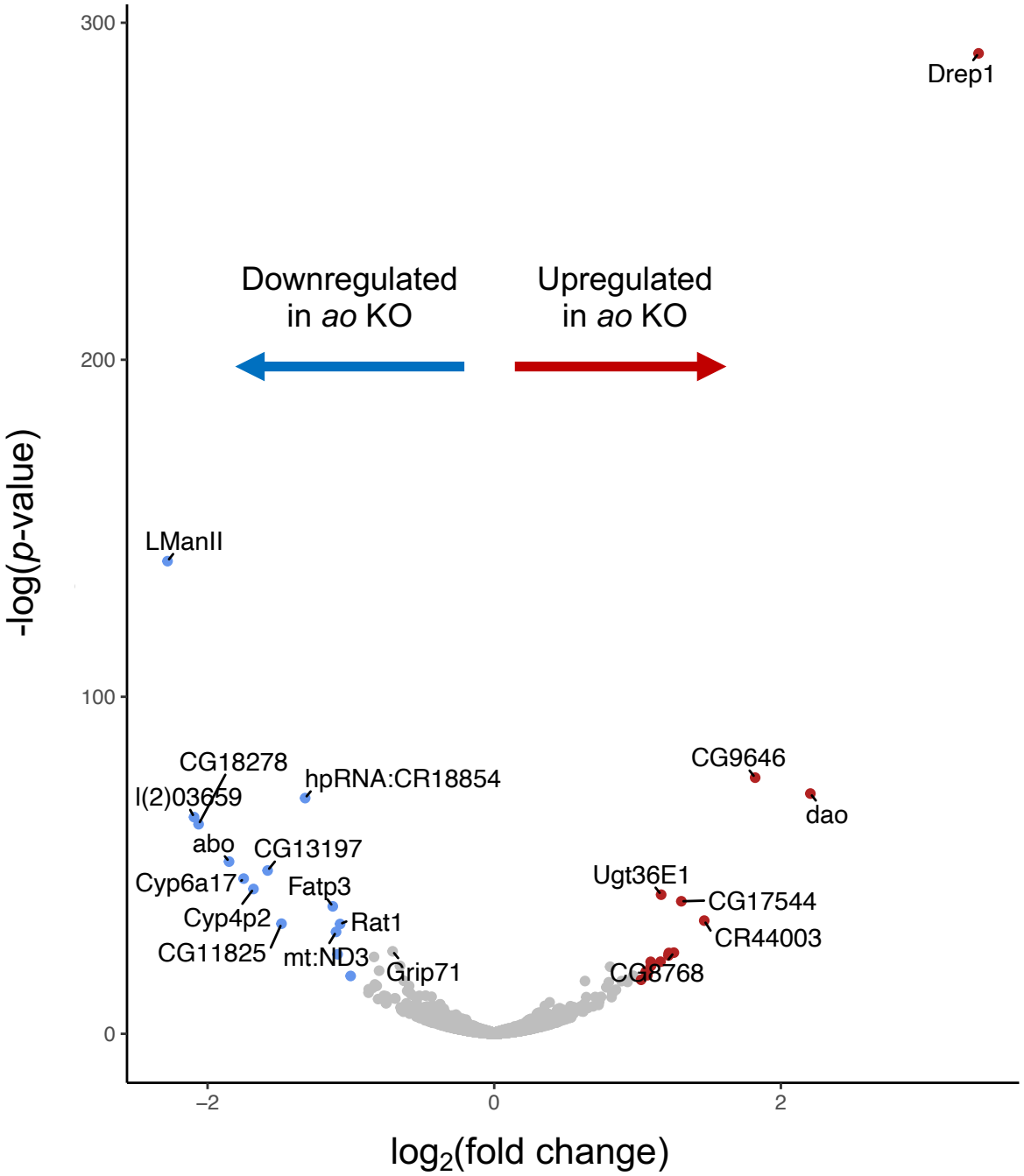

Figure A1.1: Differentially expressed genes (Δ*ao*/WT) from poly(A)-selected RNA-seq. Genes colored in blue have $\log_2$fold change < -1.0 and adjusted *p*-value < 0.05. Genes colored in red have $\log_2$fold change > 1.0 and adjusted *p*-value < 0.05. The top 20 differentially expressed genes are labeled. WT is the isogenic *yw* with wildtype *ao*.

A1.2: Methods

Sample preparation for the ribo-depletion library

We dissected ovaries from 4-day-old Δ*ao* and isogenic *yw* virgin females for RNA-seq. We prepared samples in biological triplicates for each genotype, with n=4 pairs of ovaries per replicate. For each replicate, we transferred 4 pairs of ovaries to an Eppendorf tube and homogenized the tissue in 20µL of TRIzol (Invitrogen) with a disposable pestle and electric homogenizer. The samples were stored at -80°C in 100µL of TRIzol until ready to be processed. We incubated the thawed samples in 1mL of TRIzol for 5 minutes, then centrifuged at 13,000rpm for 10 minutes at 4°C to separate the supernatant. We extracted the supernatant with chloroform and then extracted the soluble phase with isopropanol. After a wash in 70% ethanol, the RNA pellet was resuspended in RNAse-free water. The samples were treated with DNAse I (Zymo Research) and then purified with the RNA Clean & Concentrator-5 kit (Zymo Research). We quantified the purified samples with the Qubit RNA Broad Range Assay Kit (Invitrogen), then sent the RNA to Azenta Life Sciences (Burlington, MA) for ribosomal-RNA depletion library preparation and sequencing.

Sample preparation for the poly(A) selection library

Samples were prepared as above for the ribo-depletion samples, with the following differences: We dissected ovaries from 3-to-5-day old Δ*ao* and isogenic *yw* virgin females for RNA-seq. We prepared samples in biological triplicates for each genotype, with n=15 pairs of ovaries per replicate. We sent the purified RNA to Azenta Life Sciences (Burlington, MA) for poly(A)-selected library preparation and sequencing.

Data analysis

We mapped the reads to the *D. melanogaster* dm6 genome assembly using HISAT2. We used ht-seq count to count the reads (poly(A) library), bedtools to count histone reads (ribo-depletion library), and DESeq2 to detect genes differentially expressed between Δ*ao* and wildtype samples. Data analyses were performed in R (R Core Team 2024) and on Galaxy (The Galaxy Community 2024).

Appendix 2: Positive selection of *Drosophila ao*

A2.1: Summary and results

Contrary to expectation for an essential gene, there is evidence for positive selection on Ao within the *Drosophila* genus based on the McDonald-Kreitman test (Table A2.1). The McDonald-Kreitman test (McDonald and Kreitman 1991) looks for signatures of positive selection by comparing the polymorphism among populations within a species (P_n/P_s calculated as the ratio of nonsynonymous to synonymous SNPs) to the divergence between two species (D_n/D_s calculated as the ratio of nonsynonymous to synonymous substitutions). Under the null hypothesis (neutrality, or the absence of positive selection) the P_n/P_s to D_n/D_s (also known as the neutrality index, or NI) equals one. A neutrality index less than one implies evidence of positive selection (Fig A2.1).

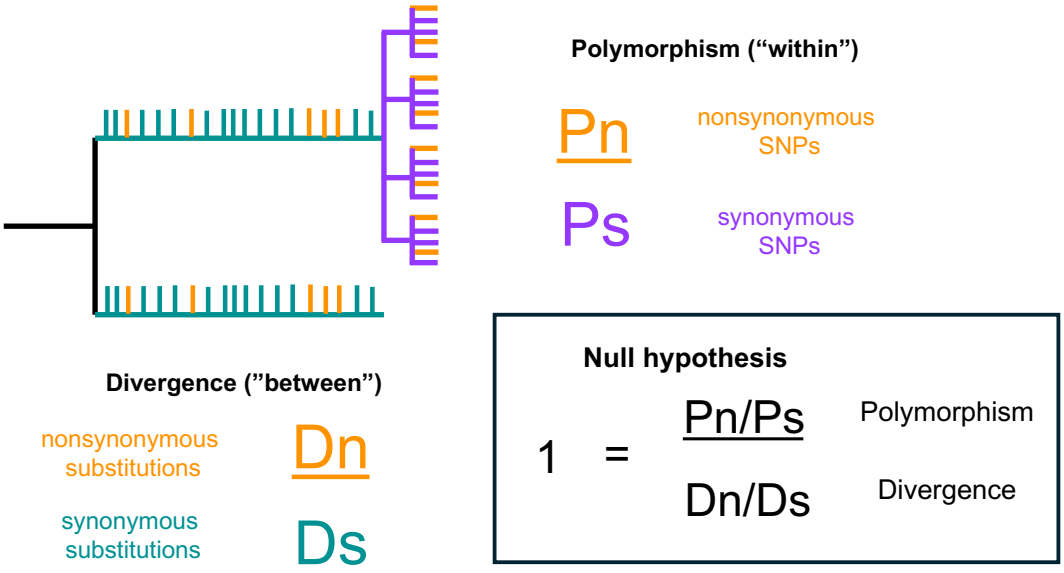

Figure A2.1: Illustration of the McDonald-Kreitman test. The MK test looks for signatures of positive selection by comparing P_n/P_s to P_n/P_s. Under the null hypothesis of neutrality, this ratio, known as the neutrality index, equals one. Neutrality index less than one indicates evidence for positive selection.

The McDonald-Kreitman test indicated that *ao* is under positive selection between *D. melanogaster* and the closely related *D. simulans* (NI=0.50, Fisher's exact test p=0.03; Table A2.1). We followed up by performing polarized McDonald-Kreitman tests between *D. melanogaster* and *D. simulans* using *D. yakuba* as an outgroup and found that the positive selection occurred along the *D. simulans* lineage (Table A2.1)

	Dn	**Ds**	**Pn**	**Ps**	**NI**	***p* (FET)**
mel vs. *sim*	25	27	62	133	0.50	0.03
Polarized *mel*	4	12	45	97	1.39	0.78
Polarized *sim*	17	10	17	36	0.28	0.02

Table A2.1: McDonald-Kreitman test on Ao. The *D. Yakuba ao* sequence was used as the outgroup for the polarized tests. *p*-value is from the Fisher's exact test.

Based on the results of the McDonald-Kreitman test, we tested whether the *D. simulans* Ao protein could rescue the loss of the *D. melanogaster* Ao *in vivo*. Using the same PhiC31 integrase approach described in Chapter 2, we engineered a *D. melanogaster* fly with the *D. simulans ao* transgene (under the *D. melanogaster ao* promoter) on the 3rd chromosome. We crossed these '*simulans-ao* rescue*'* flies into our Δ*ao* flies to obtain a *D. melanogaster* fly with a homozygous deletion of endogenous *ao* and two copies of the *D. simulans ao* on the 3rd chromosome. We performed fertility assays using these flies to test whether the *D. simulans ao* could rescue the *D. melanogaster* Δ*ao* phenotype. Contrary to our expectation based on the McDonald-Kreitman test, we found that the *D. simulans ao* transgene rescued the maternal-effect lethality of Δ*ao* flies (Fig A2.2). We conclude that despite the signature of positive selection on the Ao protein between *D. melanogaster* and *D. simulans*, the *D. simulans* Ao performs the same function as the *D. melanogaster* Ao in *D. melanogaster* flies.

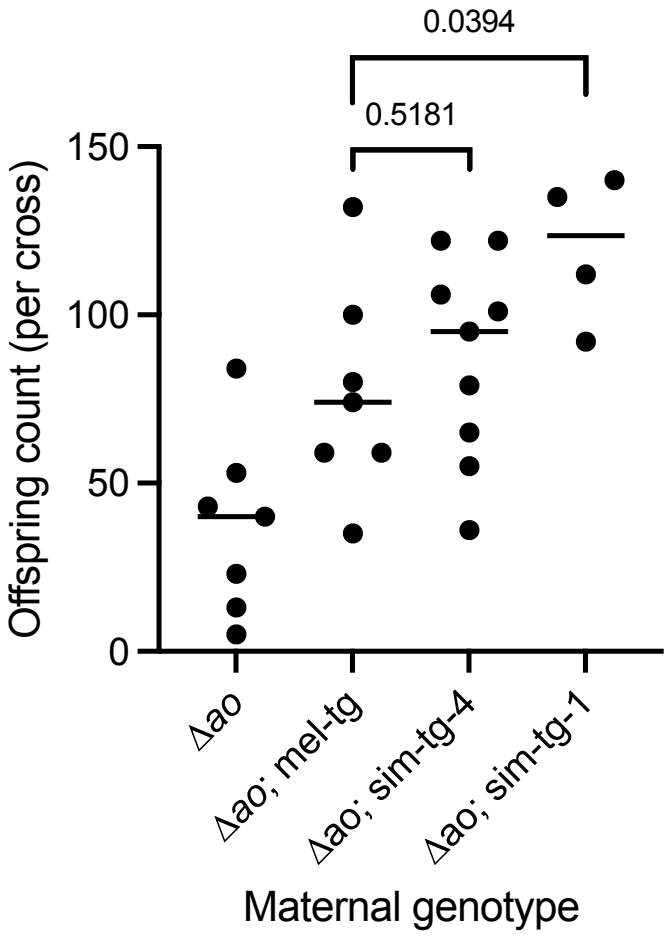

Figure A2.2: Fertility assay of Δ*ao* flies with the *D. simulans ao* transgene. Each point on a graph is the offspring count from a biological-replicate cross. All crosses plotted on one graph were set up, flipped, and counted on the same days. Crosses were set up and maintained at 29°C. Δ*ao*; mel-tg is the Δ*ao* flies with two copies of the *D. melanogaster* 'rescue' *ao* transgene on the 3rd chromosome, as described in Chapter 2. Δ*ao*; sim-tg-4 and Δ*ao*; sim-tg-4 are separate lines derived from two independent PhiC31 insertions. All females were mated to Δ*ao* males. *p*-values are from two-tailed Mann-Whitney U tests.

A2.2: Methods

McDonald-Kreitman test

We performed the McDonald-Kreitman test in R (R Core Team 2024) using the codes in Janet Young's Github repository (https://github.com/jayoung/MKtests_JY).

Generation of the *D. simulans ao* rescue line

We used the PhiC31 integrase system to create the *"*rescue" line with the *D. simulans ao*. We cloned the *ao* coding sequence from *D. simulans* with the *D. melanogaster* endogenous promoter into the pattB plasmid, which contains an *attB* site and *mini-white* marker (Bischof et al. 2013; DGRC stock 1420). BestGene Inc. midi-prepped and injected the plasmid into BDSC 9750 embryos, which have the VK33 *attP* landing site on the 3rd chromosome (Venken et al. 2006). BestGene Inc. confirmed successful integration with PCR to verify the presence of the recombined *attL* site and absence of the original *attP* site (see Table 2.2 for primer sequences), then crossed out the gene encoding the PhiC31 integrase and balanced the 3rd chromosome over *TM6B*.

Fertility assays

Flies were maintained on the benchtop at room temperature on corn syrup/soy media made in-house at Fred Hutch Cancer Center (Seattle, WA) or purchased from Archon Scientific (Durham, NC). To conduct fertility assays, we used 1-to-5-day-old males and virgin females raised at room temperature. We paired 4 virgin females with 2 males in a vial with corn syrup/soy media and allowed them to mate for 1 week at 29°C. To prevent larval overcrowding in the vials, we flipped the parents to new vials after 3 days and discarded the parents from the new vials 4 days later. We counted the adult offspring (F1) to exhaustion.

We excluded crosses with no larvae in one or both vials from statistical analyses. Because non-genetic factors, including variation in food and ambient humidity, influence fly fertility, we only compared data among the crosses set up on the same day. We used GraphPad Prism version 10.1.1 for macOS (GraphPad Software) to plot the data and conduct statistical analyses. To compare the offspring count between the two datasets, we performed two-tailed Mann-Whitney U tests and reported exact *p*-values.

REFERENCES

Bawankar, P., T. Lence, C. Paolantoni, I. U. Haussmann, M. Kazlauskiene *et al.*, 2021 Hakai is required for stabilization of core components of the m6A mRNA methylation machinery. Nature communications 12**:** 3778.

Benvenuto, G., F. Formiggini, P. Laflamme, M. Malakhov and C. Bowler, 2002 The photomorphogenesis regulator DET1 binds the amino-terminal tail of histone H2B in a nucleosome context. Current Biology 12**:** 1529-1534.

Berloco, M., L. Fanti, A. Breiling, V. Orlando and S. Pimpinelli, 2001 The maternal effect gene, abnormal oocyte (abo), of Drosophila melanogaster encodes a specific negative regulator of histones. Proceedings of the National Academy of Sciences 98**:** 12126-12131.

Bernhardt, A., E. Lechner, P. Hano, V. Schade, M. Dieterle *et al.*, 2006 CUL4 associates with DDB1 and DET1 and its downregulation affects diverse aspects of development in Arabidopsis thaliana. The Plant Journal 47**:** 591-603.

Bischof, J., M. Björklund, E. Furger, C. Schertel, J. Taipale *et al.*, 2013 A versatile platform for creating a comprehensive UAS-ORFeome library in Drosophila. Development 140**:** 2434-2442.

Brand, A. H., and N. Perrimon, 1993 Targeted gene expression as a means of altering cell fates and generating dominant phenotypes. development 118**:** 401-415.

Cavaliere, V., F. Graziani, S. Andone, A. Manzi and C. Malva, 1991 Complete reversion of the abo phenotype in D. melanogaster occurs only when the blood transposon is lost from region 32E. Molecular and General Genetics MGG 230**:** 433-441.

Chang, C.-H., and A. M. Larracuente, 2019 Heterochromatin-enriched assemblies reveal the sequence and organization of the Drosophila melanogaster Y chromosome. Genetics 211**:** 333-348.

Chari, S., H. Wilky, J. Govindan and A. A. Amodeo, 2019 Histone concentration regulates the cell cycle and transcription in early development. Development 146**:** dev177402.

Chasan, R., and K. V. Anderson, 1989 The role of easter, an apparent serine protease, in organizing the dorsal-ventral pattern of the Drosophila embryo. Cell 56**:** 391-400.

Cho, Y. S., L. M. Stevens and D. Stein, 2010 Pipe-dependent ventral processing of Easter by Snake is the defining step in Drosophila embryo DV axis formation. Current Biology 20**:** 1133-1137.

Chory, J., C. Peto, R. Feinbaum, L. Pratt and F. Ausubel, 1989 Arabidopsis thaliana mutant that develops as a light-grown plant in the absence of light. Cell 58**:** 991-999.

Chory, J., and C. A. Peto, 1990 Mutations in the DET1 gene affect cell-type-specific expression of light-regulated genes and chloroplast development in Arabidopsis. Proceedings of the National Academy of Sciences 87**:** 8776-8780.

Community, T. G., 2024 The Galaxy platform for accessible, reproducible, and collaborative data analyses: 2024 update. Nucleic Acids Research**:** gkae410.

Cook, R. K., S. J. Christensen, J. A. Deal, R. A. Coburn, M. E. Deal *et al.*, 2012 The generation of chromosomal deletions to provide extensive coverage and subdivision of the Drosophila melanogaster genome. Genome biology 13**:** 1-14.

D'Andrea, R. J., R. Stratmann, C. F. Lehner, U. P. John and R. Saint, 1993 The three rows gene of Drosophila melanogaster encodes a novel protein that is required for chromosome disjunction during mitosis. Molecular biology of the cell 4**:** 1161-1174.

Duffy, J. B., 2002 GAL4 system in Drosophila: a fly geneticist's Swiss army knife. genesis 34**:** 1-15.

El-Brolosy, M. A., Z. Kontarakis, A. Rossi, C. Kuenne, S. Günther *et al.*, 2019 Genetic compensation triggered by mutant mRNA degradation. Nature 568**:** 193-197.

El-Brolosy, M. A., and D. Y. Stainier, 2017 Genetic compensation: A phenomenon in search of mechanisms. PLoS genetics 13**:** e1006780.

Fields, S., and O.-k. Song, 1989 A novel genetic system to detect protein–protein interactions. Nature 340**:** 245-246.

Fujita, Y., G. Krause, M. Scheffner, D. Zechner, H. E. M. Leddy *et al.*, 2002 Hakai, a c-Cbl-like protein, ubiquitinates and induces endocytosis of the E-cadherin complex. Nature cell biology 4**:** 222-231.

G. Kapetanaki, M., J. Guerrero-Santoro, D. C. Bisi, C. L. Hsieh, V. Rapić-Otrin *et al.*, 2006 The DDB1-CUL4ADDB2 ubiquitin ligase is deficient in xeroderma pigmentosum group E and targets histone H2A at UV-damaged DNA sites. Proceedings of the National Academy of Sciences 103**:** 2588-2593.

Ganetzky, B., 1999 Yuichiro Hiraizumi and forty years of segregation distortion. Genetics 152**:** 1-4.

Gratz, S. J., F. P. Ukken, C. D. Rubinstein, G. Thiede, L. K. Donohue *et al.*, 2014 Highly specific and efficient CRISPR/Cas9-catalyzed homology-directed repair in Drosophila. Genetics 196**:** 961-971.

Graziani, F., L. Vicari, E. Boncinelli, C. Malva, A. Manzi *et al.*, 1981 Selective replication of ribosomal DNA repeats after loss of the abnormal oocyte phenotype in Drosophila melanogaster. Proceedings of the National Academy of Sciences 78**:** 7662-7664.

Grieder, N. C., M. d. Cuevas and A. C. Spradling, 2000 The fusome organizes the microtubule network during oocyte differentiation in Drosophila. Development 127**:** 4253-4264.

Haemer, J., 1978 Studies on heterochromatin of Drosophila melanogaster, pp. University of Washington.

Hornig, N. C., P. P. Knowles, N. Q. McDonald and F. Uhlmann, 2002 The dual mechanism of separase regulation by securin. Current biology 12**:** 973-982.

Inohara, N., and G. Nunez, 1999 Genes with homology to DFF/CIDEs found in Drosophila melanogaster. Cell death and differentiation 6**:** 823-824.

Jackson, S., and Y. Xiong, 2009 CRL4s: the CUL4-RING E3 ubiquitin ligases. Trends in biochemical sciences 34**:** 562-570.

Jäger, H., A. Herzig, C. F. Lehner and S. Heidmann, 2001 Drosophila separase is required for sister chromatid separation and binds to PIM and THR. Genes & development 15**:** 2572-2584.

Kaido, M., H. Wada, M. Shindo and S. Hayashi, 2009 Essential requirement for RING finger E3 ubiquitin ligase Hakai in early embryonic development of Drosophila. Genes to Cells 14**:** 1067-1077.

Kremer, H., and W. Hennig, 1990 Isolation and characterization of a Drosophila hydei histone DNA repeat unit. Nucleic acids research 18**:** 1573-1586.

Krider, H. M., and B. I. Levine, 1975 Studies on the mutation abnormal oocyte and its interaction with the ribosomal DNA of Drosophila melanogaster. Genetics 81**:** 501-513.

Krider, H. M., B. Yedvobnick and B. I. Levine, 1979 The effect of abo phenotypic expression on ribosomal DNA instabilities in Drosophila melanogaster. Genetics 92**:** 879-889.

Lee, J., and P. Zhou, 2007 DCAFs, the missing link of the CUL4-DDB1 ubiquitin ligase. Molecular cell 26**:** 775-780.

Leismann, O., A. Herzig, S. Heidmann and C. F. Lehner, 2000 Degradation of Drosophila PIM regulates sister chromatid separation during mitosis. Genes & development 14**:** 2192-2205.

Li, H., and R. Durbin, 2010 Fast and accurate long-read alignment with Burrows-Wheeler transform. Bioinformatics 26: 589-595.

Lifton, R., M. Goldberg, R. Karp and D. Hogness, 1978 The organization of the histone genes in Drosophila melanogaster: functional and evolutionary implications, pp. 1047-1051 in *Cold Spring Harbor symposia on quantitative biology*. Cold Spring Harbor Laboratory Press.

Lindsley, D., 1999 Larry Sandler: personal recollections. Genetics 151**:** 1233-1237.

Manzi, A., F. Graziani, T. Labella, G. Gargiulo, F. Rafti *et al.*, 1986 Changes in abo phenotypic expression without increase in rDNA in Drosophila melanogaster. Molecular and General Genetics MGG 205**:** 366-371.

Marzluff, W. F., E. J. Wagner and R. J. Duronio, 2008 Metabolism and regulation of canonical histone mRNAs: life without a poly (A) tail. Nature Reviews Genetics 9**:** 843-854.

Mazzalupo, S., and L. Cooley, 2006 Illuminating the role of caspases during Drosophila oogenesis. Cell Death & Differentiation 13**:** 1950-1959.

McDonald, J. H., and M. Kreitman, 1991 Adaptive protein evolution at the Adh locus in Drosophila. Nature 351**:** 652-654.

McKay, D. J., S. Klusza, T. J. Penke, M. P. Meers, K. P. Curry *et al.*, 2015 Interrogating the function of metazoan histones using engineered gene clusters. Developmental cell 32**:** 373-386.

Misra, S., P. Hecht, R. Maeda and K. V. Anderson, 1998 Positive and negative regulation of Easter, a member of the serine protease family that controls dorsal-ventral patterning in the Drosophila embryo. Development 125**:** 1261-1267.

Moore, G. D., D. A. Sinclair and T. A. Grigliatti, 1983 Histone gene multiplicity and position effect variegation in Drosophila melanogaster. Genetics 105**:** 327-344.

Mukae, N., H. Yokoyama, T. Yokokura, Y. Sakoyama, H. Sakahira *et al.*, 2000 Identification and developmental expression of inhibitor of caspase-activated DNase (ICAD) in Drosophila melanogaster. Journal of Biological Chemistry 275**:** 21402-21408.

Nassrallah, A., M. Rougée, C. Bourbousse, S. Drevensek, S. Fonseca *et al.*, 2018 DET1-mediated degradation of a SAGA-like deubiquitination module controls H2Bub homeostasis. Elife 7**:** e37892.

Ndoja, A., R. Reja, S.-H. Lee, J. D. Webster, H. Ngu *et al.*, 2020 Ubiquitin ligase COP1 suppresses neuroinflammation by degrading c/EBPβ in microglia. Cell 182**:** 1156-1169. e1112.

Noma, K., A. Goncharov and Y. Jin, 2014 Systematic analyses of rpm-1 suppressors reveal roles for ESS-2 in mRNA splicing in Caenorhabditis elegans. Genetics 198**:** 1101-1115.

Pappireddi, N., L. Martin and M. Wühr, 2019 A review on quantitative multiplexed proteomics. Chembiochem 20**:** 1210-1224.

Park, O. K., and H. H. Park, 2013 A putative role of Drep1 in apoptotic DNA fragmentation system in fly is mediated by direct interaction with Drep2 and Drep4. Apoptosis 18**:** 385-392.

Parry, D. M., and L. Sandler, 1974 The genetic identification of a heterochromatic segment on the X chromosome of Drosophila melanogaster. Genetics 77**:** 535-539.

Pepper, A., T. Delaney, T. Washburnt, D. Poole and J. Chory, 1994 DET1, a negative regulator of light-mediated development and gene expression in Arabidopsis, encodes a novel nuclear-localized protein. Cell 78**:** 109-116.

Petroski, M. D., and R. J. Deshaies, 2005 Function and regulation of cullin–RING ubiquitin ligases. Nature reviews Molecular cell biology 6**:** 9-20.

Philp, A. V., J. M. Axton, R. D. Saunders and D. M. Glover, 1993 Mutations in the Drosophila melanogaster gene three rows permit aspects of mitosis to continue in the absence of chromatid segregation. Journal of cell science 106**:** 87-98.

Pick, E., O.-S. Lau, T. Tsuge, S. Menon, Y. Tong *et al.*, 2007 Mammalian DET1 regulates Cul4A activity and forms stable complexes with E2 ubiquitin-conjugating enzymes. Molecular and cellular biology 27**:** 4708-4719.

Pimpinelli, S., W. Sullivan, M. Prout and L. Sandler, 1985 On biological functions mapping to the heterochromatin of Drosophila melanogaster. Genetics 109**:** 701-724.

Port, F., and S. L. Bullock, 2016 Augmenting CRISPR applications in Drosophila with tRNA-flanked sgRNAs. Nature methods 13**:** 852-854.

Port, F., H.-M. Chen, T. Lee and S. L. Bullock, 2014 Optimized CRISPR/Cas tools for efficient germline and somatic genome engineering in Drosophila. Proceedings of the National Academy of Sciences 111**:** E2967-E2976.

Ritossa, F., and S. Spiegelman, 1965 Localization of DNA complementary to ribosomal RNA in the nucleolus organizer region of Drosophila melanogaster. Proceedings of the National Academy of Sciences 53**:** 737-745.

Sandler, L., 1970 The regulation of sex chromosome heterochromatic activity by an autosomal gene in Drosophila melanogaster. Genetics 64**:** 481.

Sandler, L., 1977 Evidence for a set of closely linked autosomal genes that interact with sex-chromosome heterochromatin in Drosophila melanogaster. Genetics 86**:** 567-582.

Sandler, L., Y. Hiraizumi and I. Sandler, 1959 Meiotic drive in natural populations of Drosophila melanogaster. I. The cytogenetic basis of segregation-distortion. Genetics 44**:** 233.

Sandler, L., D. Lindsley, B. Nicoletti and G. Trippa, 1968 Mutants affecting meiosis in natural populations of Drosophila melanogaster. Genetics 60**:** 525.

Schier, A. F., 2007 The maternal-zygotic transition: death and birth of RNAs. Science 316**:** 406-407.

Schneider, I., 1972 Cell lines derived from late embryonic stages of Drosophila melanogaster. Development 27**:** 353-365.

Schroeder, D. F., M. Gahrtz, B. B. Maxwell, R. K. Cook, J. M. Kan *et al.*, 2002 De-etiolated 1 and damaged DNA binding protein 1 interact to regulate Arabidopsis photomorphogenesis. Current Biology 12**:** 1462-1472.

Shukla, H., M. Chakraborty and J. Emerson, 2024 Genetic variation in recalcitrant repetitive regions of the Drosophila melanogaster genome. bioRxiv**:** 2024.2006. 2011.598575.

Stratmann, R., and C. F. Lehner, 1996 Separation of sister chromatids in mitosis requires the Drosophila pimples product, a protein degraded after the metaphase/anaphase transition. Cell 84**:** 25-35.

Strausbaugh, L. D., and E. S. Weinberg, 1982 Polymorphism and stability in the histone gene cluster of Drosophila melanogaster. Chromosoma 85**:** 489-505.

Sullivan, W., and S. Pimpinelli, 1986 The genetic factors altered in homozygous abo stocks of Drosophila melanogaster. Genetics 114**:** 885-895.

Sullivan, W. T., 1985 Heterochromatic elements which function early in Drosophila embryogenesis, pp. University of Washington.

Tautz, D., J. M. Hancock, D. A. Webb, C. Tautz and G. A. Dover, 1988 Complete sequences of the rRNA genes of Drosophila melanogaster. Molecular biology and evolution 5**:** 366-376.

Tomkiel, J., L. Fanti, M. Berloco, L. Spinelli, J. W. Tamkun *et al.*, 1995 Developmental genetical analysis and molecular cloning of the abnormal oocyte gene of Drosophila melanogaster. Genetics 140**:** 615-627.

Tomkiel, J., S. Pimpinelli and L. Sandler, 1991 Rescue from the abnormal oocyte maternal-effect lethality by ABO heterochromatin in Drosophila melanogaster. Genetics 128**:** 583-594.

Venken, K. J., Y. He, R. A. Hoskins and H. J. Bellen, 2006 P [acman]: a BAC transgenic platform for targeted insertion of large DNA fragments in D. melanogaster. Science 314**:** 1747-1751.

Waizenegger, I. C., J. F. Giménez-Abián, D. Wernic and J.-M. Peters, 2002 Regulation of human separase by securin binding and autocleavage. Current biology 12**:** 1368-1378.

Wang, H., L. Zhai, J. Xu, H.-Y. Joo, S. Jackson *et al.*, 2006 Histone H3 and H4 ubiquitylation by the CUL4-DDB-ROC1 ubiquitin ligase facilitates cellular response to DNA damage. Molecular cell 22**:** 383-394.

Wang, Y., L. Zhang, H. Ren, L. Ma, J. Guo *et al.*, 2021 Role of Hakai in m6A modification pathway in Drosophila. Nature communications 12**:** 2159.

Wertz, I. E., K. M. O'Rourke, Z. Zhang, D. Dornan, D. Arnott *et al.*, 2004 Human De-etiolated-1 regulates c-Jun by assembling a CUL4A ubiquitin ligase. Science 303**:** 1371-1374.

White, A. E., B. D. Burch, X.-c. Yang, P. Y. Gasdaska, Z. Dominski *et al.*, 2011 Drosophila histone locus bodies form by hierarchical recruitment of components. Journal of Cell Biology 193**:** 677-694.

Wolf, J. B., and M. J. Wade, 2009 What are maternal effects (and what are they not)? Philosophical Transactions of the Royal Society B: Biological Sciences 364**:** 1107-1115.

Yanagawa, Y., J. A. Sullivan, S. Komatsu, G. Gusmaroli, G. Suzuki *et al.*, 2004 Arabidopsis COP10 forms a complex with DDB1 and DET1 in vivo and enhances the activity of ubiquitin conjugating enzymes. Genes & development 18**:** 2172-2181.

Yedvobnick, B., H. M. Krider and B. I. Levine, 1980 Analysis of the autosomal mutation abo and its interaction with the ribosomal DNA of Drosophila melanogaster: the role of X-chromosome heterochromatin. Genetics 95**:** 661-672.

Yokoyama, H., N. Mukae, H. Sakahira, K. Okawa, A. Iwamatsu *et al.*, 2000 A Novel Activation Mechanism of Caspase-activated DNase fromDrosophila melanogaster. Journal of Biological Chemistry 275**:** 12978-12986.

Yuan, K., C. A. Seller, A. W. Shermoen and P. H. O'Farrell, 2016 Timing the Drosophila mid-blastula transition: a cell cycle-centered view. Trends in Genetics 32**:** 496-507.

Zhang, W., X. Zhang, Z. Xue, Y. Li, Q. Ma *et al.*, 2019 Probing the function of metazoan histones with a systematic library of H3 and H4 mutants. Developmental cell 48**:** 406-419. e405.

Zhao, S., Y. Zhang, R. Gamini, B. Zhang and D. Von Schack, 2018 Evaluation of two main RNA-seq approaches for gene quantification in clinical RNA sequencing: polyA+ selection versus rRNA depletion. Scientific reports 8**:** 4781.